91602
new 82-10

COMPLIMENTARY COPY
Please Credit Ontario Hydro Research if Reproduced in Whole or in Part.

ontario hydro
research division

# DESIGN CONSIDERATIONS FOR SEALING THE SHAFTS OF A NUCLEAR FUEL WASTE DISPOSAL VAULT

Report No 85-13-K

M.H.S. Mortazavi
H.T. Chan
H.S. Radhakrishna
Engineers
Civil Research Department

## ABSTRACT

The shafts in an underground disposal system, which constitute potential pathways between the disposal vault and the biosphere, should be effectively sealed if the system is to perform as a hydrodynamic and geochemical barrier for the safe containment of nuclear fuel waste. In the design of the shaft backfill, consideration should be given to ensure that the backfill and the backfill/rock interface remain intact. Design-related problems, including critical pathways for the transport of radionuclides, configuration of shaft backfill and its functional requirements, the state of stress in a backfilled shaft with particular emphasis on the arching and load transfer phenomenon are discussed in this report.



| job | file | date | report no. |
|---|---|---|---|
| 740643-104-461 | 843.2 | May 3, 1985 | 85-13-K |

TABLE OF CONTENTS


| | | Page |
|---|---|---|
| 1.0 | INTRODUCTION | 1 |
| 2.0 | CRITICAL FLOW PATHWAYS IN A BACKFILLED SHAFT | 2 |
| | 2.1 Potential Flow Paths in a Backfilled Shaft | 2 |
| | 2.2 Movement of Radionuclides | 3 |
| 3.0 | CONFIGURATION OF SHAFT SECTION AND STRESS CONDITIONS IN ROCK AROUND THE SHAFT | 5 |
| | 3.1 Stress Variations Around Shafts | 5 |
| | 3.2 Conceptual Design Schemes for Shaft Sealing | 7 |
| 4.0 | FUNCTIONAL REQUIREMENTS OF SHAFT BACKFILL | 7 |
| | 4.1 Hydraulic Conductivity of Backfill Materials | 9 |
| | 4.2 Sorption Capacity | 10 |
| | 4.3 Deformation and Compatibility | 11 |
| 5.0 | LATERIAL AND SWELLING PRESSURES IN BACKFILLED SHAFT | 12 |
| | 5.1 Backfill Weight and Lateral Pressure | 12 |
| | 5.2 Swelling Pressures | 13 |
| 6.0 | STATE OF STRESS AND PHYSICAL INTEGRITY OF BACKFILLED SHAFT | 15 |
| | 6.1 State of Stress in Backfill | 16 |
| | 6.2 Physical Integrity of the Backfilled Shaft | 22 |
| 7.0 | SUMMARY | 24 |
| REFERENCES | | 26 |
| DISTRIBUTION | | last page |

91602
new 82-10

ontario hydro
research division

To: Mr. H.N. Isaac
Manager
Nuclear Materials Management
Department
Design & Development Division

Attn: Mr. T.J. Carter

# DESIGN CONSIDERATIONS FOR SEALING THE SHAFTS OF A NUCLEAR FUEL WASTE DISPOSAL VAULT

## 1.0 INTRODUCTION

An option which is being considered by the Atomic Energy of Canada Limited (AECL) for the long-term disposal of nuclear fuel waste is the isolation of the radioactive waste in plutonic rock at about 1000 m below the ground surface. In the design of such an underground disposal vault, adequate isolation of the nuclear fuel waste from the biosphere must be ensured for a long period of time. To meet this requirement, the shafts, drifts and disposal caverns must be sealed with suitable materials in such a way as to ensure that they do not form easy pathways for the migration of radionuclides which could be ultimately released from the waste container to the biosphere. As part of Ontario Hydro's Technical Assistance Program (TAP) to AECL, a study on shaft sealing was undertaken in the Soil Sciences Section of the Research Division.

It is assumed for the purpose of this study that at the completion of waste disposal and vault backfilling, the access shafts would be backfilled with a compacted clay mixed with a filler material such as sand or crushed granite. Clays and clay-based materials are favoured for their low hydraulic conductivity, low ionic diffusivity and long-term geochemical compatability with the host rock.

A part of this study is devoted to the collection of data on the physical properties of clay backfills, on the lateral and swelling pressures in the emplaced backfill and on the stresses in the rock adjacent to the shaft opening/1/. Based on the

published data, an analysis was made of the vertical stress distribution in the backfill and at the backfill rock interface in a backfilled shaft. It was hypothesized that a well-compacted and intact backfill in a shaft should have hydraulic conductivity low enough to ensure that the transport of radionuclides would be by a diffusion process. However, some conditions may exist in a shaft backfill to affect its physical integrity, such as cracks developed in the emplaced backfill mass due to differential compression, and separation at the interface of the rock and backfill due to high hydraulic pressures /2,3/.

In this study, a preliminary analysis of the state of the stresses in the constructed backfill showed that the vertical stress would be much less than the values imposed by the self weight of the backfill because of friction and adhesion developed at the backfill rock interface. The reduction of vertical and horizontal stresses in the backfill may become critical as the ground water pressure in the rock around the shaft is developed with time. The ground water pressure, if it is high, may reduce the effective stress in the shaft backfill to less than zero, a condition for cracks or separation to develop within the backfill mass or in the interfacial zone respectively.

The critical pathways for ground water flow carrying radionuclides as well as for the movement of radionuclides through the backfilled shaft are briefly discussed in Section 2. The various conceptual design schemes for shaft sealing and the stress conditions in the host rock in various shaft opening geometries and the degree and extent of excavation-induced damage in the host rock are described in Section 3. Functional requirements of the shaft backfill and physical and geochemical properties of compacted backfill are included in Section 4. The major stress components in the constructed backfill, the factors controlling their magnitude, and the ground water induced effects on the physical integrity of the shaft backfill are discussed in Sections 5 and 6. A summary of the main points is presented in Section 7.

## 2.0 CRITICAL FLOW PATHWAYS IN A BACKFILLED SHAFT

In this section the critical flow paths for ground water carrying radionuclides through a backfilled shaft are identified and a brief discussion is made on the migration of radionuclides through the shaft backfill.

### 2.1 Potential Flow Paths in a Backfilled Shaft

The flow pattern of ground water at a disposal site is governed by the natural regional ground water regime, the flow caused by

the construction of a disposal vault, and the flow induced by radiogenic heat and osmotic gradients. The resultant ground water flow pattern would therefore depend on site conditions and the design of the disposal facility. For the purpose of the present study, it is assumed that the induced thermal gradients are large enough to cause an upward flow of ground water through the backfilled shaft(s).

Figure 1 shows a summary of the environmental conditions likely to be present in a disposal vault due to natural and induced effects.

Ground water flow through the backfilled shafts depends on the following factors:

(1) the regional ground water flow,

(2) the radiogenic heat induced thermal gradients and their buoyancy effect on ground water, and

(3) the water bearing strata and zones of differential hydrostatic pressures intercepted by the vertical shafts.

Regional ground water flow is predominantly horizontal or subhorizontal. Superimposed on this would be the effects of radiogenic heat induced upward flow and the vertical flow between two aquifiers. Figure 2 shows the three parallel pathways for ground water movement through a backfilled shaft. Figure 3 indicates the significance of fissure width and spacing in rock to ground water flows/4/. The ground water can flow either through the backfilled zone, or backfill-rock interface or the damaged zone in the rock surrounding the shaft. The flow will predominate in the least resistant of these three pathways.

In order that the shaft backfilling be effective, the potential for the formation of cracks in the backfill and separation between the backfill and rock should be prevented. Also the fractures in the rock surrounding the shaft backfill should be effectively sealed to prevent ground water flow.

## 2.2 Movement of Radionuclides

As an aqueous fluid migrates through the geosphere, certain reactions occur which are dependent upon the chemistry of the migrating fluid and the chemistry and geochemistry of other fluids and solid phases with which it comes in contact. These geochemical reactions determine the relative rate at which the species in the migrating fluid travel with respect to the advancing front of water. Historically the generic term "sorption" has been applied to describe these geochemical reactions which include ion exchange, adsorption, precipitation, complex formulation, oxidation-reduction reactions and precipitate filtration of colloids.

The retardation of radionuclide mobility in the geosphere, including the backfilled excavations, is largely determined by the ion exchange sites on the solid phase which is primarily governed by the amount of net electrical charge at the surface. This is one of the significant factors influencing the selection of clay-based materials for sealing and backfilling of the disposal vault excavations.

Based on the simplified mathematical model for solute transport in saturated porous media, the effect of geochemical reactions on the transport process of radionuclides through the backfill and the host rock can be assessed by the experimental determination of the sorption coefficients $K_d$ and $K_a$ respectively, provided the experimental conditions adequately simulate the predicted environmental conditions in the geosphere.

Due to the ion-exchange and adsorption mechanisms, the solute ions move more slowly than the ground water by a factor called the retardation factor, ie:

$$\bar{V}_{i(p)} = \bar{V}_p / R_d = \bar{V}_p / (1 + K_d \, \rho / n) \text{ for porous media and}$$

$$\bar{V}_{i(f)} = \bar{V}_f / R_a = \frac{1}{12s} \frac{\rho_w g}{\mu} \frac{e^4}{e + 2K_a} I \text{ for fractured media}$$

(Snow's model)

where:

$$K_d = \frac{q_A}{C_a} = \frac{\text{concentration of substance adsorbed on solid material (solute mass/unit mass of medium)}}{\text{concentration of substance in aqueous phase (solute mass/unit volume of solution)}} \quad (L^3/M),$$

$$K_a = \frac{q_a}{C_a} = \frac{\text{solute mass per unit area of solid phase}}{\text{solute concentration in solution}}, \quad (L)$$

$V_i$ = average migration velocity of radionuclide i

$V_p$ = average flow velocity in porous medium

$V_f$ = average flow velocity in fractured medium

$R_d$ = retardation factor for porous media

$R_a$ = retardation factor for fractured media

$s$ = spacing of fractures

$e$ = aperture of fracture

$\rho$ = bulk density of geologic medium

$n$ = porosity of porous medium

$\mu$ = viscosity of the permeant

$\rho_w$ = density of the permeant

$I$ = resultant hydraulic gradient

Among the parameters controlling the magnitude of retardation factors, the density/porosity of the porous media and the fracture opening of the fractured media are the major factors influencing the retardation process besides the media's intrinsic properties and environmental conditions represented by $K_d$ and $K_a$ values for any species of radionuclides (see Figure 4).

An approximate measure of one-dimensional travel times for the radionuclides can be estimated as $t_p = Z/V_{i(p)}$ and $t_f = Z/V_{i(f)}$ in porous and fractured media respectively, where Z is the depth of the disposal vault from the biosphere, (p) and (f) denote the porous and fractured media respectively.

## 3.0 CONFIGURATION OF SHAFT SECTION AND STRESS CONDITIONS IN ROCK AROUND THE SHAFT

In this section the stress conditions in the host rock around the shaft opening for different configurations are discussed. It is seen that an understanding of the stress conditions in the rock wall is important because the extent of the excavation-damaged zone is partly dependent on the state of stresses in the rock and this damaged zone around the shaft wall can be a critical pathway for the escaping radionuclides from the waste source to the biosphere.

### 3.1 Stress Variations Around Shafts

The main factors controlling the size and shape of the shafts are: operational requirements, shaft sinking technology, equipment and procedures.

The degree of disturbance in the host rock caused by shaft sinking operations depends largely on the degree of anisotropy, concentration of in situ stresses, the shape of the shaft opening and the method of excavation. The extent of the

disturbed zone on the other hand is primarily influenced by the size of the opening.

Based on the plane strain solution for a perfectly elastic medium, Figure 5 shows the stress conditions around a shaft with circular or elliptical cross section for different states of in situ stresses from the "Kirsch Solution"/5,6/. Table I gives the stress concentrations for various shapes of openings under a uniaxial stress field. The stress concentrations corresponding to other stress fields can be determined by the method of superimposition.

As seen from Figure 5, the tangential stress ($\sigma_t$) at the perimeter of the shaft does not vary with its size whereas the amount of the ground subjected to the increased tangential stress is proportional to the size of the shaft. When the in-situ horizontal stress is not uniform in all directions due to residual stress fields and/or anisotropic conditions, the shape of a shaft can significantly influence the type and amount of tangential stress (compare Figures 5c with Figure 5b).

It should be noted that the theoretical analysis presented above is only approximate due to the assumption of a two-dimensional plane-strain condition disregarding the confinement effect of gravity which can be significant in the case of vertical shafts. Most rocks are considerably strengthened by confinement. For example, in the case of granitic rock with an average value of $\phi = 45°$, failure cannot occur above a principal stress ratio of $R_s = 0.17$ ($\sigma_1 = q_u/1\text{-}R_s \tan^2 (45 + \phi/2)$, where $R_s = \sigma_3/\sigma_1$). However, the rock may show plastic or viscous behaviour at very high stresses resulting in a relaxed zone around the shaft being probably fissured or micro-fractured.

Many researchers have presented various relationships for in situ stresses with respect to depth and mechanical properties of rock. The existence of high horizontal stresses has been shown to be a global phenomenon. So long as elastic behaviour is assumed and original horizontal confinement remains, the high horizontal stress will also be preserved. One area of research work in AECL's Underground Research Laboratory (URL) in Lac du Bonnet, Manitoba is intended to provide information on the in situ stresses and mechanical properties of rock to be employed in the evaluation of their influences on the Canadian disposal vault design features.

A significant factor controlling the quality of the rock surrounding the shaft is the excavation method. Present tunnelling technology indicates that a suitable size shaft (e.g. by tunnel boring machine, TBM) can be produced with minimum amount of

damage to the surrounding rock by taking into consideration the strength and hardness of the rock as well as the shape and alignment of the shaft. Advanced methods of tunnelling, such as by rock fusion, water jetting, etc may become practical by the time of repository construction.

Based on the above discussion, several precautionary measures can be considered to decrease the degree and extent of disturbance around the shaft opening/1/. These include:

(1) selection of the smallest possible size of opening,

(2) selection of the shape of opening to produce the most favourable stress distribution in the host rock around the shaft,

(3) application of a method of excavation which produces the least amount of damage to the walls of the shaft and the surrounding rock,

(4) application of internal pressure (back-pressure) in order to decrease the tangential stress at the perimeter of the shaft, and

(5) prevention of rock surface weathering during the preclosure period of the repository by the use of the New Austrian Tunnelling Method (NATM) approach to support the ground and observe its behaviour during this period/7/.

Most of the above measures are site-dependent. However, a circular opening appears to be the most desirable shape satisfying many of the requirements pertaining to the seal's functional objectives. Since the shaft penetrates the various geologic formations and features, design alterations should be considered at important locations in order to isolate a permeant producing zone and enhance the seal-rock compatability.

### 3.2 Conceptual Design Schemes for Shaft Sealing

Some of the preliminary conceptual design schemes suitable for shaft sealing are summarized in Table II. These may be grouped into two major categories; the homogeneous backfill system and the multiple seal/backfill system. Advantages and disadvantages of each specific scheme are also summarized in Table II.

## 4.0 FUNCTIONAL REQUIREMENTS OF SHAFT BACKFILL

The primary functions of shaft backfilling are: (i) to mitigate the permeant fluid movement toward and through the disposal vault, and (ii) to retard the migration of radionuclides from

the geosphere to the biosphere. To fulfill these primary functions, the backfill should have the following attributes:

(1) low hydraulic conductivity,

(2) adequate sorption capacity to retard migration of radionuclides having a wide range of physiochemical characteristics, and

(3) compatability with host rock and ground water conditions to maintain physical integrity within the backfill and at the backfill/rock interfacial zone.

The performance of the shaft backfill will be influenced by the design features and the preclosure and post-closure environmental conditions. The major factors among these conditions are: the rock surface conditions, the ground water conditions (hydraulic pressure), and the ground water-rock-backfill physiochemical interactions.

Considering a simplified flow model as shown in Figure 2, the total flux in the axial direction of the backfilled shaft is given by:

$$Q_t = k_s A_s + k_i A_i + k_d A_d$$

where $k_s$, $k_i$ and $k_d$ are the hydraulic conductivity of backfill mass, backfill rock interface and fractured (damaged) host rock respectively and $A_s$, $A_i$ and $A_d$ are their corresponding areas perpendicular to the flow path. $k_s$ depends on a number of intrinsic properties of the backfill material and the environmental factors such as temperature, pressure and the permeant chemistry. $k_s$ can be measured in the laboratory and the parameters governing its magnitude can be evaluated. $k_d$ depends on aperture, size and filling, frequency and orientation of both natural and newly formed fractures by the shaft penetration. The hydraulic conductivity of the fractured rock has to be measured by in situ testing. The hydraulic conductivity of the backfill rock interface ($k_i$) is governed by the deformation behaviour of the backfill with respect to the host rock. The velocity of upward flow and hence the migration of radionuclides from the disposal vault through the backfilled shaft is controlled by the most permeable zone. Therefore it is important to select an impervious backfill and ensure an intimate contact between the backfill and rock and to seal effectively the damaged zone in the rock.

Geologic materials are regarded as the most likely candidates for backfilling of the disposal vault excavations because of (1)

our knowledge about their properties and behaviour in the geological time scale and their compatability with host media under natural environmental conditions, (2) history of their long-term behaviour and stability, and (3) economic advantage and their abundance in nature/1,2/.

In the following subsections, the important properties of backfill materials will be discussed and data on soil properties will be presented. It is believed that this type of information will be useful for the design of shaft backfills using compacted clay soils. Also, the collected data are useful in analyzing the stresses in the shaft backfill which is part of the present study.

## 4.1 Hydraulic Conductivity of Backfill Materials

The relationship between the hydraulic conductivity and the properties of soil and the permeant fluid is expressed by the Kozeny-Carman equation for laminar flow in porous medium based on Poiseuille's equation for flow through round capillary tubes/8/. These mathematical expressions have been found to be satisfactory in the case of porous media with approximately uniform pores and equidimensional particles such as sands. However, in the case of many clay soils, they are found inadequate due to the influence of soil fabric and interactions of the permeant fluid with plate-like clay particles/9/. The relatively large macropores (intracluster) and the small micropores (intercluster), as well as their variations in size and shape under different environmental conditions, can influence considerably the hydraulic conductivity of a fine-grained medium/10/.

Deviations occur from Darcy's law of fluid flow through porous media when the hydraulic gradient is smaller than the threshold value or larger than the critical value. In the former case, the effects of an opposite osmotic flow, viscosity of mineral-adsorbed water being higher than that of surface-distant pore water, and clogging of flow paths by migrating particles will dominate the fluid flow. In the latter case, flow anomalies may be caused by the channelling effect of erosion even in highly densified fine-grained soils.

The following are some of the important factors which control the hydraulic conductivity of compacted soils:

(1) The pore size and the pore geometry which, for a particular soil type, are determined by the particles mass continuity being, in turn, primarily a function of soil's bulk density (Figure 6).

(2) The effects of temperature and time, as shown in Figure 7, which are mainly due to changes in the permeant fluid properties such as viscosity and soil-water interactions and volume changes respectively/11/.

(3) The fabric of the compacted soil controlled by factors such as: compaction characteristics (see Figure 8), compositional properties including interlayer bonds, ion-exchange capacity, type of exchangeable ions, and pore fluid chemistry (Figures 8 and 9).

Results of various hydraulic conductivity tests on different backfill materials from a literature survey and recent experimental work related to disposal vault sealing programs are compiled as given in Tables III to VII.

Based on the above discussion, the factors controlling the hydraulic conductivity of compacted clays should be considered in the evaluation of potential backfill materials for their hydrodynamic barrier quality by some type of permeability test/12/.

The type of test, method of testing, and the associated sources of errors can have significant effects on the measured value of k. It is very important to carry out the tests under circumstances which represent the actual field conditions as closely as possible.

As shown in Figure 2, the hydraulic conductivity of the backfill/rock interface, $k_i$, depends on the integrity (or separation) of the interfacial zone which, in turn, is controlled by the volume change characteristics and compressibility of the emplaced backfill with the host rock.

## 4.2 Sorption Capacity

The process of sorption-retardation and its contribution to the chemical barrier quality of the disposal vault backfill has been briefly explained in Section 2.2 of this report. The high sorption capability and low hydraulic conductivity, among the factors discussed earlier in this section, justify the selection of a clay-based material as backfilling and sealing materials for the shafts of a disposal vault.

Table VIII presents a summary of the $k_d$, bulk sorption coefficient, values reported in the literature for different radionuclides under various pH and chemical compositions of the solution phase/13/, and Table IX presents the recommended ranges of $k_d$ for crushed granite as well as the surface sorption

coefficient, $k_a$, for granite rock or rock fracture surfaces for the commonly anticipated conditions of the solution phase/14/.

## 4.3 Deformation and Compatability

In order for the backfilled shafts to perform satisfactorily the emplaced backfill should maintain its physical integrity both within its mass and at the interface contacts with the host rock. Otherwise, channelling and bypassing could reduce the travel times of escaping radionuclides through the backfilled shaft.

Therefore, in the design of the shaft backfills, the deformation properties of the backfill and its compatability with the host rock should be considered.

The structural integrity of the shaft backfill largely depends on its deformation characteristics and the state of stress within the backfill mass and at the backfill/rock interfacial zone throughout the design life of the disposal vault.

The major factors which control the structural integrity of shaft backfill are their compressibility and volume change behaviour. The amount of compression/expansion and the resistance to volume change depends on both the compositional factors and the environmental conditions.

The compositional factors include: type and amount of each mineral, type, size and volume of adsorbed cations, mineral lattice structure (geometry and charge), shape and size distribution of particles, and pore fluid chemistry. These factors primarily manifest themselves in the bulk density, plasticity and type of fabric of soils. On these bases, it is anticipated that the compressibility and volume change of clay minerals increase in the order of kaolinite < illite < montmorillonite.

The environmental conditions include: the opening geometry and host rock surface conditions, the compaction effort (input energy), molding water content, ground water, its availability, pressure and chemistry, temperature and geologic events. These factors require careful considerations for the design of effective backfills.

Table X gives a summary of the requirements and geotechnical characteristics of a shaft backfill material.

## 5.0 LATERAL AND SWELLING PRESSURES IN BACKFILLED SHAFT

Disruption of the physical integrity of the backfilled shaft may be caused by the formation of macro-discontinuities in the backfill due to compression under its own weight and arching action in a long column of backfill. Other forms of disruption could be by uplift of the backfill mass near the ground surface, extrusion of the swelling clay backfill into the host-rock fractures and separation of the backfill/rock interface by "hydraulic compression"/15/.

The major sources of stress components in the backfill are its self weight and corresponding lateral pressure, lateral pressure due to compaction, adhesive bond stress, and swelling pressures (horizontal and vertical components). In the following subsections, a discussion of the lateral and swelling pressures and the factors controlling their magnitudes is included. The ground water pressure conditions around the shaft backfill are site dependent and are not discussed in this report.

### 5.1 Backfill Weight and Lateral Pressure

The backfill weight is a function of its density which is controlled by the compaction effort and moisture content for a selected backfill material. It should be noted that the density and moisture content of the backfill may change by compression under its own weight during construction and in the post-closure period. These changes may cause variations in other stress components such as lateral and swelling pressures, which are also controlled by the availability of ground water and the development of hydrostatic pressure with time. It is very important to predict reasonably well the ground water flow regime and the consequent pore-fluid pressures in the backfill for the analysis of the state of effective stress.

Considering that the walls of a shaft in the granitic rock of the Canadian Shield are rigid and unyielding, the lateral stress in the backfill is predominantly in an "at-rest" condition. Results of earlier investigations by Terzaghi and Tschebotarioff have shown that the at-rest earth pressure coefficient $K_o$ is strongly affected by the wall friction, consolidation of the backfill, and the degree of support rigidity for both cohesionless and cohesive backfills.

The angle of wall friction, $\delta$, between the compacted backfill and the host rock, depends on the rock surface roughness, the density and moisture content of the backfill, and the relative movement between the backfill and the rock. Similarly, the adhesive bond between the backfill and the rock, $c_a$, is

controlled by the backfill's cohesion, degree of saturation, rock surface conditions and temperature (Figure 10).

Table XI gives a summary of historical data on the "at rest" earth-pressure coefficient $K_o$. Figure 11 shows the relationships between $K_o$ and other basic soil parameters obtained for natural soil deposits/16/.

When the backfill material is emplaced in the shaft by compaction, a lateral pressure is exerted on the shaft walls. In evaluating the development of this compaction lateral pressure during compaction of the backfill, as shown in Figure 12a, the following three zones could be differentiated/17/:

(1) the zone where the influence of compaction is fully acting and the lateral pressure due to compaction is:

$$p_c = \gamma K_v d_v$$

where: $d_v$ = thickness of this zone
$k_v$ = compaction lateral pressure coefficient
and $\gamma$ = bulk density of soil,

(2) the zone where the compaction effect decreases to zero, and

(3) the zone where there is no influence due to compaction.

Figures 12b and 12c show the building up of the lateral pressure due to compaction assuming that the backfill is compacted behind a rigid, unyielding wall in layers of $d_v$ thickness.

The effect of the degree of compaction on the magnitude of $k_v$ should be considered in relation to the $K_o$ value. The greater the compaction effort, the higher the backfill density but the lower the $K_o$ value. Therefore, as shown in Figure 12, the total lateral pressure of a backfill compacted by a high or very high compactive effort is only slightly larger than that of a backfill compacted by a medium compactive effort, presumably due to an arching or silo effect.

## 5.2 Swelling Pressures

One of the ways to ensure a positive seal at the rock/backfill interface is to use a material with a potential to swell. This swelling potential can be advantageous to enhance the physical integrity of backfilled excavations in the disposal vault. This can be achieved by the development of swelling of the material upon contact with water and under the confinement of the surrounding host rock, if it results in an overall compressive state of effective stress.

Therefore, it is important to understand the factors controlling the swelling pressure components in the backfill. These are briefly discussed as follows.

The swelling mechanism of clay soils may be considered in terms of both mechanical and physio-chemical components contributing to the interparticle equilibrium. The physico-chemical component of swelling has been analyzed by many authors (eg Mitchell/9/, Yong and Warkentine/18/, etc) by using the concept of osmotic pressure and the diffuse-double layer theory. It should be noted that these relationships are not simple and reliable for quantitative estimation of swelling pressure, especially if no experimental verification is possible. Furthermore, in this theory, based on colloidal suspensions, the effects of attractive forces and anions are not considered, and thus the theory predicts unlimited expansion whereas there appears a limit on expansion of all clays.

The major compositional and environmental factors which govern the swelling behaviour of clay soils are their clay mineral composition, (Figures 13 and 14), the soil fabric and the pore fluid chemistry.

The influence of soil fabric, expressed in terms of initial density, initial water content and surcharge loads, on swelling pressure has been investigated by Yevnin and Zaslavsky/19/. The results of about 161 tests carried out on statically compacted samples of an alluvial clay soil (62% < 0.002 mm consisting of 60% Ca-montmorillonite, 14% kaolinite and 13% illite) with 56 different combinations of factors are summarized in Figures 15 and 16. Similar correlations should be established for the candidate backfill material in order to predict the variations in swelling pressure and bulk density under emplacement conditions.

In their investigation, Yevnin and Zaslavsky/19/ measured the swelling pressures after 5 days when the samples were found to be 100% saturated and the swelling pressure remained nearly constant after this period. However, in the case of shaft backfilling, the influence of time may be more important depending on the availability of water, the ground water regime, and the migration of a wetting front in the backfill/15/.

Considering the significant effect that the soil fabric and confining pressure have on the swelling pressure development, it is to be expected that the swelling pressures will exhibit anisotropy. Furthermore because of the non uniform availability of water along the backfilled shaft, large variations in the magnitude and rate of development of swelling pressures could be

expected. These factors should be considered in the assessment of the swelling performance of backfills and seals.

The process of hydration and swelling in the backfill may affect its physical properties such as hydraulic conductivity, deformability and strength.

The effect of swelling on the hydraulic conductivity of compacted clay soil is dependent on its moisture level in relation to the optimum moisture content. For soils compacted at moisture contents on the dry side of the optimum value, the swelling has a greater effect on hydraulic conductivity. For soils compacted at moisture contents on the wet side of the optimum value, the swelling potential is relatively small and the soil fabric (degree of particles parallelism) controls the hydraulic conductivity (Figure 8). The greater the dispersivity of the clay particle, the smaller the hydraulic conductivity up to a certain water content, beyond which the interparticle distances start to increase causing more rapid migration of water resulting in a greater hydraulic conductivity.

The volume change behaviour of clay soils is controlled by two mechanisms. In the first mechanism, the compressibility is controlled by the shearing resistance of the particle's contact points and volume changes occur by shear displacement and/or sliding between particles. In the second mechanism, compressibility is governed by the long-range electrical forces at the solid-liquid interfaces such as the double layer repulsive forces. Experimental results have indicated/20/ that mechanism 1 primarily controls volume change behaviour in non-swelling lattice-type clays like kaolinites. However, in swelling lattice-type soils, like montmorillonite clays, mechanism 2 controls the compressibility which is resisted by repulsive force or swelling pressure.

High swelling pressures may cause uplifting of the seal and/or backfill mass in the shaft. This may be critical in the uppermost part of the shaft where the swelling pressure could exceed the downward vertical confining pressure by the weight of backfill and side adhesion between the backfill and rock.

## 6.0 STATE OF STRESS AND PHYSICAL INTEGRITY OF BACKFILLED SHAFT

Compacted soil backfills are compressible materials and compression is a stress- and time-dependent behaviour. The host rock surrounding the backfilled excavations can be considered as being infinitely stiff and unyielding compared to the backfill. Compression of the backfill in a shaft can occur by self-weight and ground water pressure build up with time. In the case of

rapid redevelopment of ground water pressure, if the in-flow fluid pressure were greater than the lateral soil pressure, the "impervious" compressible backfill would compress laterally and an opening would develop between the rock and backfill. The process is referred to as "hydraulic compression"/15/.

For a satisfactory performance of the backfill as a barrier against the vertical flow of water carrying radionuclides, an intimate contact between the backfill and rock wall is necessary.

The potential for separation of the shaft backfill from the rock wall by hydraulic compression depends upon the following factors in the post-closure period:

(1) the magnitude of ground water pressure developed at the backfill-rock interface,

(2) the rate of ground water pressure development in relation to the rate of penetration of ground water into the backfill,

(3) the lateral earth pressure at the backfill-rock interface, and

(4) the compressibility and swelling potential of the compacted backfill.

The magnitude and rate of ground water pressure development are site dependent, while the lateral earth pressure, the hydraulic conductivity, and the compressibility or swelling are time-dependent properties of the shaft backfill.

The complex interaction of the above time-dependent parameters should be considered in the design of the shaft backfilling and sealing system/2/.

In this section an approximate analysis is made to indicate the factors influencing the state of stress in the backfilled shaft with emphasis on the arching effect and the possibility of hydraulic fracturing and/or hydraulic compression during various stages of backfill performance.

## 6.1 State of Stress in Backfill

The backfill shaft can be considered as an unyielding silo in which the vertical stress distribution will be greatly influenced by the shear stresses developed along the wall of the shaft as the backfill compresses under its own weight. If no separation occurs along the interfacial zone, the soil will hang

on the shaft wall. This process of load transfer is commonly called an arching or silo action.

According to the classical theories of arching/21/, the vertical stress in the backfill along the depth of the shaft increases less rapidly than the weight of the backfill and approaches asymptotically a finite value.

A simplified analytical solution for the vertical stress distribution can be derived by rewriting Janssen equations in terms of effective stresses and using the following assumptions:

(1) the shaft wall is infinitely rigid,

(2) vertical stresses are constant and uniform in horizontal planes,

(3) the ratio of effective lateral to vertical stress (Ko) is constant with depth,

(4) the backfill/rock interface is the surface of sliding and the vertical stress in the yielding part of backfill is equal to the difference between the weight of backfill above the section and the shear resistance (or $S_b$ = bond stress) along the interface.

If $S_b$ does not fully develop to the shearing strength along the interface then $S_b = \frac{\tau}{F} = (c'_a + \sigma'_h \tan\delta)/F$

where: $\tau$ = shear strength
$c'_a$ = effective cohesion of backfill
$\sigma'_h$ = effective horizontal pressure
$\delta$ = frictional angle
$F$ = shearing mobilization factor

$$\sigma'_h = P_{s(h)} + (\sigma_h - u)$$

where: $P_{s(h)}$ = horizontal component of swelling pressure
$\sigma_h$ = total horizontal pressure
$u$ = pore pressure

Since placing of the backfill is considered spontaneous, it is assumed that backfill construction will proceed without consolidation and pore pressure, u, will be related to $\sigma_v$ (vertical pressure); therefore:

Assuming that the rate of backfilling is rapid, the "end of construction" pore pressure is as follows:

$$u = u_o + \bar{B}\sigma_v$$

where: $u_o$ = pore pressure immediately after backfill placement

$\bar{B}\sigma_v$ = change in pore pressure accompanying a change in vertical stress from 0 to $\sigma_v$

$$\therefore \quad (\sigma_h - u) = K_o(\sigma_v - u) = K_o(\sigma_v - u_o - \bar{B}\sigma_v) = K_o(\sigma_v(1-\bar{B}) - u_o),$$

(5) changes in vertical component of swelling pressure is neglected and the horizontal component of swelling pressure $P_{s(h)}$ is assumed constant with depth,

(6) the constructed backfill is uniform in density, and

(7) lateral pressure due to compaction of backfill is considered negligible.

Figure 17 represents a column of backfill in a circular shaft, of radius a, which is settling under its own weight. The condition that the sum of the vertical stress components, which act on the slice and must be equal to zero, can be expressed as follows:

$$\pi a^2 \gamma dz = \pi a^2 (\sigma_v' + d\sigma_v') - \pi a^2 \sigma_v' +$$

$$2\pi a \left\{\frac{P_{s(h)}\tan\delta + (c_a' + K_o(\sigma_v(1-\bar{B}) - u_o)\tan\delta)}{F}\right\} dz$$

$$\text{or} \quad \frac{d\sigma_v'}{dz} = \gamma - \frac{2}{a}\left\{\frac{P_{s(h)}\tan\delta + [K_o(\sigma_v(1-\bar{B}) - u_o)\tan\delta + c_a']}{F}\right\}$$

where: $\tan\delta$ = frictional coefficient between backfill and shaft rock-wall surface

$c_a'$ = the adhesion at the interfacial zone

$\gamma$ = unit weight of backfill
$P_{s(h)}$ = horizontal component of swelling pressure
$K_o$ = at rest earth pressure coefficient
$\bar{B}$ = pore pressure coefficient
F = shearing mobilization factor

By integrating this equation with boundary conditions that $\sigma_v = 0$ when $z = 0$

$$\sigma_v' = \frac{1}{A}[\gamma - \frac{2}{Fa}(c_a' + P_{s(h)} \tan\delta - u_o K_o \tan\delta)](1-e^{-Az}) - u_o$$

where: $A = \dfrac{[2K_o \tan\delta(1-\bar{B})]}{Fa}$

and $\sigma_h' = \sigma_v' K_o$

In the long-term case where the backfill is saturated,

$$\sigma_v' = \frac{1}{A'}[\gamma - \frac{2}{Fa}(c_a' + P_{s(h)} \tan\delta - K_o u \tan\delta)](1-e^{-A'z}) - u$$

where $A' = \frac{2}{Fa} K_o \tan\delta$

In order to show the effect of the primary factors controlling the stresses in the backfilled shaft, the above equations are simplified first by neglecting the effects of adhesion, swelling pressure and pore water pressure. Therefore:

$$\sigma_v' = \frac{Fa}{2K_o \tan\delta} \gamma (1-e^{-\frac{2}{Fa} \cdot Z \cdot K_o \cdot \tan\delta})$$

which in non-dimensional form is

a) $$\frac{\sigma_v'}{\gamma Z} = \frac{F}{4r_1 r_2 K_o \tan\delta}(1-e^{-4Fr_1 r_2 K_o \tan\delta}) \; ; \; \frac{\sigma_h'}{\gamma Z} = K_o \frac{\sigma_v'}{\gamma Z}$$

or

b) $$\frac{\sigma_v'}{\gamma Z} = \frac{FR}{K_o \tan\delta}(1-e^{-Fr_3 K_o \tan\delta}) \; ; \; \frac{\sigma_h'}{\gamma Z} = K_o \frac{\sigma_v'}{\gamma Z}$$

where:

$$r_1 = \frac{H}{D}\ , \text{ aspect ratio}$$

$$\left.\begin{aligned} r_2 &= \frac{Z}{H} \\ r_3 &= \frac{Z}{R} \end{aligned}\right\} \text{depth ratios}$$

where: H = height of backfill between two rigid elements, such as bulkheads
D = shaft diameter
R = hydraulic radius of shaft cross section (area/perimeter)

From the above equations, which are similar to Janssen's formula/21/, it is seen that the non-dimensional stress components are primarily influenced by:

a) the shearing strength mobilization factor, F, and the coefficient of friction at the backfill-rock wall interface, $\tan\delta$, which may vary with depth (and displacement).

b) the backfill constraints along the shaft depth, if provided by rigid structural elements such as bulkheads, in terms of aspect ratio and depth ratios. This factor is closely related to the assumption (ii) made in the above analysis, and

c) the shape factor or hydraulic radius of the shaft cross section which indicates increasing arching effect with decreasing hydraulic radius of the shaft section. For example, in a shaft with a square cross section, the arching effect is greater than in a circular shaft with the same cross-sectional area; similarly, the smaller the size of the shaft, the greater is the reduction in compressive stresses due to arching action.

Also, the secondary parameters such as backfill/rock interface adhesion, $c_a$, swelling pressure of backfill, and pore water pressure have significant influence on the stress components in the backfilled shaft. The influences of some of these factors on the state of stress are illustrated by the following numerical example in which the required soil parameters are assumed as follows:

Partially Saturated Backfill

$\gamma$ = 18 kN/m$^3$

$P_{s(h)}$ = 0, (swelling pressure is ignored)

$\bar{B}$ = 0.25(0 to 0.5 for Proctor optimum water content)

$u_o$ = 50 kPa, assumed constant

$\delta$ = 15°

$K_o$ = 0.50

F = 1.0

Figure 18 shows the vertical stress distribution with depth based on the above assumed parameters. At depths below 30a, the vertical stress is virtually independent on the depth (Z) irrespective of the shaft size.

Experimental investigations for cohesionless backfills/21/ have shown that below the depths of 4a to 6a, the shearing resistance is fully active. The overlying backfill, thus, acts as a surcharge. It is also indicated that $K_o$ changes with depth in the upper part of the backfill, where no shearing resistance is developed and the state of stress is essentially hydrostatic in nature.

Based on the above considerations, the equations for the state of stress may be rewritten as follows:

if $Z_o = n_o a$ depth of hydrostatic zone, then $q = n_o a \gamma$. Introducing this value in the previous equation yields:

$$\sigma_v' = \frac{1}{A}\left[\gamma - \frac{2(c_a - P_{s(h)}\tan\delta - u_o K_o \tan\delta)}{Fa}\right](1-e^{-AZ'}) + qe^{-AZ'}$$

where: $A = \dfrac{2K_o \tan\delta(1-\bar{B})}{Fa}$

$Z'$ = depth below $Z_o$

Similarly, the equation for $\sigma_v'$ may be rewritten for the case of a fully saturated backfill:

$$\sigma_v' = \frac{1}{A'}\left[\gamma - \frac{2(c_a' + P_{s(h)}\tan\delta - K_o u \tan\delta)}{Fa}\right](1-e^{A'z}) + q^{-A'Z'}$$

where: $A' = \frac{2K_o \tan\delta}{Fa}$

The above analyses indicate that vertical compressive stresses are appreciably reduced due to the arching load transfer from the backfill to the shaft rock wall. Similar observations have been made by many researchers on the arching and internal load transfer from a thin (particularly vertical) clay core of earth-fill dams to rock-fill shells due to differential settlement. Results of analyses by finite element methods and field measurements in zoned dams such as Gepatsch (in Austria), Hytteju·et (in Norway), Balderhead (in England) and Holle-Harspranget (in Sweden), (see Table XII and Figures in Appendix C) support the theory of arching and load transfer from a compressible zone to relatively incompressible zones or walls in contact. A close examination of the state of effective stress in the backfill, in the context of the arching phenomenon by some modified arching theory applicable to confined conditions under consideration is therefore warranted. Further studies are required to modify and/or determine the sensitivity of the results of the above analysis particularly with respect to the material properties and environmental conditions such as: heterogeniety, anisotropy, boundary conditions (and deformations), and changes of material properties and behaviour with time.

The results of a simplified analysis presented in this report clearly indicate that the reduction of compressive stresses in the backfill due to arching is primarily governed by the geometry of the shaft cross section, the backfill-rock wall interfacial adhesion, the degree of shearing mobilization and the backfill properties such as $K_o$ and $\bar{B}$, which are related to the molding water content.

## 6.2 Physical Integrity of the Backfilled Shaft

As noted in the previous sections, the physical integrity of the backfill in a shaft is strongly dependent on the state of stress and volume change behaviour of the emplaced backfill, assuming that the host rock is relatively unyielding.

The physical integrity of the emplaced backfill, with respect to its attributes for effective sealing of the shaft, may be degraded by the formation of a separation of the backfill-rock interface, and/or cracks within the backfill mass due to hydraulic compression or hydraulic fracturing and inelastic behaviour of the backfill at various stages of the disposal vault operation.

It is, therefore, important to evaluate the performance of the emplaced backfill in the context of time-dependent boundary conditions/15/.

The following three distinct stages can be considered:

(i) End of Construction Stage (Figure 19 (a))

At this stage the backfill has been compacted in the shaft. Depending on the location of the bulkhead (if there are any), the length of the backfill column will vary. Due to the axial compression of the backfill and the arching effect, the vertical stresses in the backfill would be less than the total self-weight of the material. The full ground water pressure in the host rock is not yet acting on the backfill and the construction pore water pressure in the backfill would be negative or small. There is little swelling in the backfill, even if the backfill were to contain swelling type minerals. At this stage, the state of effective stress everywhere in the backfill would be, most likely, compressive. There should be no cracks in the backfill mass or separation between the backfill and the host rock.

(ii) Transition Stage - Ground Water Pressure Build-up (Figure 19 (b))

After a certain period of time, the full ground water pressure would be acting on the circumference of the shaft backfill. This may cause lateral compression of the backfill with the potential danger of a small gap developing at the backfill/rock interface. The potential development of the gap at the interface depends on the following factors: the magnitude of the hydraulic pressure, the compressibility of the backfill, the rate of water migration from the interface towards the centre of the backfill, the swelling potential of the backfill when its water content is increased and the lateral pressure of the backfill on the host rock. Some of these processes will be the subject of future laboratory investigations by Ontario Hydro.

If cracks have been previously developed within the backfill, they would be the critical flow paths for the ground water to penetrate into the fill. If the ground water pressure is high and the total stresses in the soil are relatively small, the effective stress components could be reduced to zero, resulting in more cracks caused by hydraulic fracturing.

It is believed that this stage is a critical one in terms of the physical integrity of the shaft backfill.

(iii) Long-Term Case - Backfill "Flooded" by Ground Water (Figure 19 (c)).

The ground water in the host rock and in the backfill has reached the equilibrium condition. The backfill is saturated and the deformation/compression of the backfill is complete. If the backfill is properly designed and constructed, the swelling of the material should close up the gaps at the soil/rock interface as well as any cracks which may be present within the backfill mass. It is important to ensure that these macro-discontinuities are closed up within a certain time period before the radionuclides migrate through the shaft backfill.

## 7.0 SUMMARY

From the study of various conditions related to shaft sealing, a number of conclusions are made as follows:

(1) A circular cross section of the shaft seems the most desirable shape which satisfies many of the requirements pertaining to the seal performance.

(2) Three critical paths for the transport of radionuclides in a sealed shaft are: vertical cracks which may be present within the emplaced backfill mass, the interface between the seal and rock wall and the excavation-damaged zone in the host rock around the shaft. Therefore it is important that no cracks be induced in the backfill, an intimate contact of the soil/rock interface be ensured and the fractures in the damaged rock zone be effectively sealed by grouting.

(3) A great deal of information is available on the properties and behaviour of compacted soil backfills which may be used for sealing a shaft. However, there are comparatively less data on the interaction and mechanistic behaviour between the soil and the rock wall as a time function.

(4) Theoretically, the vertical stress component in a column of shaft backfill does not increase linearly with its depth. Below a certain depth, the stress would remain almost constant with depth due to the arching and load transfer phenomenon at the backfill/rock interface. Since the contact pressure between the soil and the rock partly depends on the vertical stress in the soil, the reduction of the vertical stress would affect the contact pressure between the soil and the rock wall.

(5) To maintain a tight contact at the soil/rock interface, the radial compression of the shaft seal by hydraulic pressure should be less than the radial stress (primarily swelling pressure) in the soil. Both compression and swelling are complex and time-dependent processes. A mathematical model would be required to optimize these offsetting processes. This in turn would aid in ensuring that the emplaced backfill remains sufficiently intact and maintains an intimate contact with the shaft walls.

Reviewed by:

T.J. Carmichael
Supervising Engineer
Soils Section & AECL/TAP Coordinator
Civil Research Dept

Approved by:

T.W. Klym
Manager
Civil Research Dept

Prepared by:

M.H.S. Mortazavi
Engineer
Soils Section

H.T. Chan
Engineer
Soils Section

H.S. Radhakrishna
Engineer
Soils Section

MHS/HTC/HSR:kk

REFERENCES


1. M.H.S. Mortazavi, A Study of Sealing the Shafts of a Nuclear Waste Repository System, M. Eng. Project, Department of Civil Engineering, University of Toronto, September, 1982.

2. M.H.S. Mortazavi and T.C. Kenney, Study of Possible Systems and Materials for Sealing Underground Disposal Vaults for Nuclear Fuel Waste, Department of Civil Engineering, University of Toronto, October, 1983.

3. T.C. Kenney, Study of Procedures to Design Seals for Rooms, Drifts, and Shafts of Underground Nuclear Fuel Waste Vaults, Research Proposal Submitted to AECL-WNRE, Department of Civil Engineering, University of Toronto, May, 1983.

4. I. Neretnicks, Retardation of Escaping Nuclides from a Final Depository, KBS-TR-30, 1977.

5. D.F. Coates, Rock Mechanics Principles, Energy, Mines and Resources Canada, Monograph 874 (Revised 1981).

6. R.E. Goodman, Introduction to Rock Mechanics, John Wiley & Sons, 1980.

7. M.H.S. Mortazavi, New Austrian Tunnelling Method, Literature Survey, Department of Civil Engineering, University of Toronto, April, 1982, Unpublished.

8. D.W. Taylor, Fundamentals of Soil Mechanics, John Wiley & Sons, 1948.

9. J.K. Mitchell, Fundamentals of Soil Behaviour, John Wiley & Sons, Inc, 1976.

10. R. Pusch, Permeability of Highly Compacted Bentonite, KBS-80-16, 1980.

11. R.E. Olsen and D.E. Daniel, Field and Laboratory Measurement of the Permeability of Saturated and Partially Saturated Fine-grained Soils, June, 1979, Geot Eng Report GR80-5, Dept of Civil Engineering, University of Texas, Austin, Texas.

12. H.S. Radhakrishna and H.T. Chan, Laboratory Study of Physical Properties of Clay Buffers for a Nuclear Fuel Waste Vault, Conference Proc, Int, Conference on Radioactive Waste Management, CNS, September 12-15, 1982.

13. H.T. Chan, A Comparative Study of Clay-type Grouting Materials, AECL TR-231, February, 1984.

14. T.T. Vandergraaf, A Compilation of Sorption Coefficients of Radionuclides on Granites and Granitic Rock, AECL TR-120, May, 1982.

15. M.H.S. Mortazavi, Arching Effect and Hydraulic Compression in Backfilled Excavations, AECL-Vault-Sealing Workshop December 2-3, 1983, Toronto, Canada.

16. E.W. Brooker and H.O. Ireland, Earth Pressures at Rest Related to Stress History, Can. Geotech J., Vol. II, No.1, February, 1965.

17. DIN 1055(German Standards), Part 2, "Design Loads for Buildings, Soil Properties, Unit Weight, Shear Resistance and Wall Friction", Translated from German by B. Lewicki, 1974.

18. R.N. Yong and B.P. Warkentin, Introduction to Soil Behavior, MacMillan, 1966.

19. A. Yevnin and D. Zaslavsky, Some Factors Affecting Compacted Clay Swelling, Can Geotech. J. Vol. 7, 1970.

20. A. Sridharun and G.V. Rao, Mechanisms Controlling Volume Change of Saturated Clays and the Role of the Effective Stress Concept, Geotechnique, Vol. 23, No. 3, 1973.

21. K. Terzaghi, Arching in Ideal Soils, Ch. V, Theoretical Soil Mechanics, 1943.

TABLE I

STRESS CONCENTRATION AROUND OPENINGS UNDER UNIAXIAL STRESS FIELD**

| Shape | Height/Width | Stress Concentration ($\sigma_t$/Sy)* | |
|---|---|---|---|
| | | Point A* | Point B* |
| Ellipse | 1/2 | 5.0 | -1.0 |
| Oval | 1/2 | 3.4 | -0.9 |
| Rectangle (round corners) | 1/2 | 2.5 | -0.9 |
| Circle | 1 | 3.0 | -1.0 |
| Ellipse | 2 | 2.0 | -1.0 |
| Oval | 2 | 1.6 | -0.9 |
| Rectangle | 2 | 1.7 | -1.0 |

*see Figure 5(b) in which $S_x = 0$

**R.E. Goodman, *Introduction to Rock Mechanics*, John Wiley & Sons, 1980

## TABLE II
## VARIOUS CONCEPTUAL DESIGN SCHEMES FOR SHAFT SEALING

| DESIGN SCHEME | ADVANTAGES | DISADVANTAGES | REFERENCE |
|---|---|---|---|
| 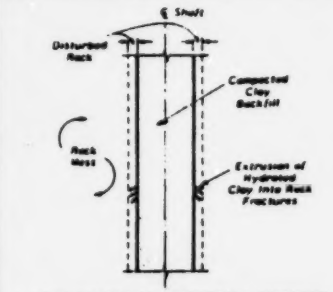 <br>1 - ONE "BACKFILL-MATERIAL" CONCEPT | - lower construction cost<br>- ease of material quality control (one material)<br>- more uniform behaviour of seal mass and seal-rock interaction | - low reliability in seal performance requirements<br>- incomplete sealing of disturbed rock | AECL TR-145 |
| 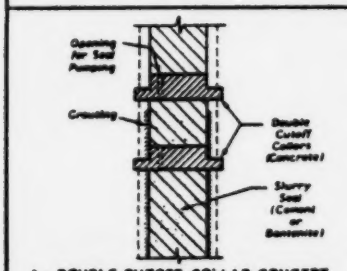 <br>2 - DOUBLE CUTOFF-COLLAR CONCEPT | - ease of backfilling<br>- reasonable sealing of disturbed rock | - longevity of cutoff collars is questionable<br>- long-term integrity of seal (backfill) may be degraded by its compression and volume change<br>- incomplete sealing of cutoff collars - problem of sealing collars opening<br>- loss of backfill due to incomplete sealing of surrounding rock<br>- very low reliability | Backfilling Practice in Mining Industry, OECD Workshop, and AECL TR145 |
| 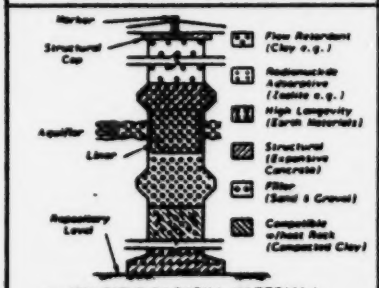 <br>3 - MULTIPLE BACKFILL MATERIAL/ GEOMETRY CONCEPT | - very high overall reliability in the seal to satisfy long-term stringent performance requirements<br>- more effective sealing of the disturbed rock and permeant-producing zones | - difficult and costly construction procedure and quality control of various materials<br>- physical integrity of the long seal section with uniform geometry is questionable<br>- very much site-dependent | D'Appolonia Design Approach, ONWI-55, USA Concept (salt-bedded or salt-dome formations) |
| 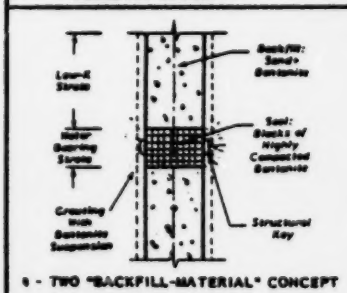 <br>4 - TWO "BACKFILL-MATERIAL" CONCEPT | - high cation exchange capacity and small hydraulic conductivity<br>- higher reliability in intersection of permeant-producing zones along the shaft<br>- reasonable quality control of the formulated material (sand + bentonite) | - higher construction cost<br>- backfill may have the seal's required properties<br>- long-term physical integrity of backfill and seal is questionable<br>- the concept seems highly over-designed in relation to CEC and K requirements<br>- high compaction of bentonite blocks and their placement in the shaft are practically questionable | KBS, General Technical Report, Swedish Concept, and AECL TR-145 |
| 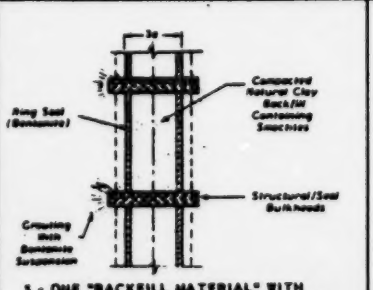 <br>5 - ONE "BACKFILL MATERIAL" WITH STRUCTURAL/SEALING BULKHEADS | - reasonably low construction cost<br>- higher compatability of backfill and bulkheads with host rock<br>- better long-term physical integrity<br>- effective sealing all along shaft length | - difficulty in quality control of natural clay<br>- possibly lower cation exchange capacity and higher hydraulic conductivity of natural clay deposits in comparison with formulated materials | M. Mortazavi and T.C. Sweeny (Granitic formations) |

References Cited in Table II

G.W. Bird and D.J. Cameron, Vault Sealing Research for the Canadian Nuclear Fuel Waste Management Program. Atomic Energy of Canada Ltd (AECL) TR-145, 1982.

OECD-NEA, Geological Disposal of Radioactive Waste, Research in the OECD Area, May, 1982.

D'Apollonia Consulting Engineers, Repository Sealing Design Approach, ONWI-55, 1979.

KBS Report, Handling and Final Storage of Unreprocessed Spent Nuclear Fuel, December 1977.

M. Mortazavi and T.C. Kenney, Study of Possible Systems and Materials for Sealing Underground Disposal Vaults for Nuclear Fuel Waste, Dept of Civil Engineering, University of Toronto, Oct 1983.

## TABLE III

## HYDRAULIC CONDUCTIVITY OF NATURAL CLAYEY SOILS
## (From Literature Survey)

| Clayey Soils | Dry Density ($g/cm^3$) | Type of Test | Hydraulic Conductivity (cm/s) | References |
|---|---|---|---|---|
| Field and laboratory compacted clays of Prairie Provinces, Canada<br>Alluvial & Glacial clays | | | $0.5 \times 10^{-6}$ to $0.5 \times 10^{-9}$ | P.J. Rivard and T.E. Goodwin (1978) |
| Clay Soils: | | | | |
| Bradwell | | percolation | $4.5 \times 10^{-9}$ | Skempton & Henkel (1960) |
| Lyndhurst | | consolidation | $1.2 \times 10^{-9}$ | Skempton & Henkel (1960) |
| Avonmouth | | percolation | $4.2 \times 10^{-7}$ | Raymond & Azzouz (1969) |
| Brown Clay | | consolidation | $3.0 \times 10^{-7}$ | |
| Blue Clay | | consolidation | $1.7 \times 10^{-6}$ | |
| Silty Clays | | | | |
| pismo | | consolidation | $(1.1\text{-}2.0) \times 10^{-8}$ | Weber (1968) |
| Lafayette | | consolidation | $(5.5\text{-}40) \times 10^{-9}$ | Weber (1968) |
| La Trianon | | consolidation | $(1.2\text{-}2.8) \times 10^{-7}$ | Weber (1968) |
| Prudehaa | | consolidation | $(2.7\text{-}18) \times 10^{-8}$ | Wilkinson (1968) |
| Fiddler's Ferry | | consolidation | $1.1 \times 10^{-8}$ | Al-Dhahir, Kennard and Morgenstern (1969) |
| Malaya | | consolidation | $1.0 \times 10^{-7}$ | James (1970) |
| Sarnia, Ontario | | percolation | $2.1 \times 10^{-8}$ | Goodall and Quigley (1977) |
| | | consolidation | $1.5 \times 10^{-8}$ | Goodall and Quigley (1977) |
| Sandy (& silty) Clays | | | | |
| pismo | | consolidation | $6.9 \times 10^{-9}$ | Weber (1968) |
| Atascadero (& silty) | | consolidation | $3.9 \times 10^{-8}$ | Weber (1968) |
| Clay Backfills | | | | |
| Balderhead, clay fill | | percolation | $1.0 \times 10^{-8}$ | Bishop and Al-Dhahir (1969) |
| M6, clay fill | | percolation | $3.4 \times 10^{-8}$ | Bishop and Al-Dhahir (1969) |
| Selset, core clay | | percolation | $7.7 \times 10^{-8}$ | Bishop and Al-Dhahir (1969) |
| Selset, found clay | | consolidation | $3.8 \times 10^{-9}$ | Bishop and Al-Dhahir (1969) |
| Diddington, core clay | | consolidation | $1.2 \times 10^{-8}$ | Bishop and Al-Dhahir (1969) |
| Diddington, found clay | | consolidation | $4.0 \times 10^{-9}$ | Bishop and Al-Dhahir (1969) |

P.J. Rivard and T.E. Goodwin, Geotechnical Characteristics of Compacted Clays for Earth Embankments in the Prairie Provinces, Can Geotech Journ, Vol 15, 1978.

A.W. Skempton and D.J. Henkel, Field Observations of Pore Pressures in London Clay. Pore Pressure and Suction in Soils. Institution of Civil Engineers, London, pp 81-84.

G.P. Raymond and M.M. Azzouz, Permeability Determination for Predicting Rates of Consolidation, Proc Conf on In Situ Investigations of Soils and Rocks, British Geot Soc, London, pp 195-203.

W.G. Weber, In Situ Permeabilities for Determining Rates of Consolidation, Hwy Research Records No 243, pp 49-61.

W.B. Wilkinson, Constant Head In Situ Permeability Tests in Clay Strata. Geotechnique, Vol 18, No 2, pp 172-194.

Z.A. Al-Dhahir, M.F. Kennard, and N.R. Morgenstern, Observations of Pore Pressures Beneath the Ash Lagoon Embankments at Fiddlers Ferry Power Station. In Situ Investigations in Soils and Rocks, Inst of Civil Engineers, London, pp 265-276.

P.M. James, The Behaviour of a Soft Recent Sediment Under Embankment Loadings. Quat J of Eng Geol, Vol 3, No 1, pp 41-53.

D.C. Goodall and R.M. Quigley, Pollutant Migration from Two Sanitary Landfill Sites Near Sarnia, Ontario. Can Geot J, Vol 14, No 2, pp 223-236.

A.W. Bishop and Z.A. Al-Dhahir, Some Comparisons Between Laboratory Tests, In Situ Tests and Full Scale Performance with Special Reference to Permeability and Coefficient of Consolidation. In Situ Investigation in Soil and Rocks, Institution of Civil Eng, London, pp 251-264.

## TABLE IV

HYDRAULIC CONDUCTIVITY OF COMPACTED BENTONITE AND BENTONITE SAND MIXTURES
(From Literature Survey)

| Material | Specimen Characteristics | | Testing Conditions | | | | Hydraulic Conductivity cm/s | References & Remarks |
|---|---|---|---|---|---|---|---|---|
| | Dry Density $g/cm^3$ | M.C. % | Temp °C | Hyd. Grad. i | Test Duration (hrs) | Type of Test | | |
| 1. Na-Bentonite (Wyoming MX-80, GS 2.7) 85% - 2 um of which 80-90% is montmorillonite | 1.90 | 46 | 20 | $10^4$ | | percolation | $2.2\times10^{-11}$ | R. Pusch, (1978, 1979) (References listed at the end of this table) |
| | | | | $5\times10^3$ | | | $2.0\times10^{-11}$ | |
| | | | | $2\times10^3$ | | | $1.9\times10^{-11}$ | |
| | | | | $10^3$ | | | $1.3\times10^{-11}$ | |
| | 1.95 | 46 | 20 | $10^4$ | | | $2.3\times10^{-11}$ | |
| | | | | $5\times10^3$ | | | $2.0\times10^{-11}$ | |
| | | | | $2\times10^3$ | | | $1.9\times10^{-11}$ | |
| | | | | $10^3$ | | | $1.5\times10^{-11}$ | |
| | | | | $10^4$ | | | $1.2\times10^{-11}$ | |
| | | | | $5\times10^3$ | | | $1.0\times10^{-11}$ | |
| | | | | $2\times10^3$ | | | $9\times10^{-12}$ | |
| | | | | $10^3$ | | | $6\times10^{-12}$ | |
| | | | | $10^4$ | | | $2\times10^{-12}$ | |
| | | | | $2\times10^3$ | | | $2\times10^{-12}$ | |
| | | | | $5\times10^3$ | | | $3.8\times10^{-11}$ | |
| | | | | $2\times10^3$ | | | $3.6\times10^{-11}$ | |
| | | | | $10^3$ | | | $3.4\times10^{-11}$ | |
| | | | | $10^4$ | | | $7\times10^{-11}$ | |
| | | | | $2\times10^3$ | | | $6\times10^{-11}$ | |
| | | | | $10^3$ | | | $5\times10^{-11}$ | |
| | | | | $10^4$ | | | $1.8\times10^{-11}$ | |
| | | | | $5\times10^3$ | | | $1.8\times10^{-11}$ | |

TABLE IV (cont'd)

HYDRAULIC CONDUCTIVITY OF COMPACTED BENTONITE AND BENTONITE SAND MIXTURES
(From Literature Survey)

| Material | Specimen Characteristics | | Testing Conditions | | | | Hydraulic Conductivity cm/s | References & Remarks |
|---|---|---|---|---|---|---|---|---|
| | Dry Density g/cm$^3$ | M.C. % | Temp °C | Hyd. Grad. i | Test Duration (hrs) | Type of Test | | |
| 2. Ca-Bentonite (Erbsloh) 85%-2 um of which 80-90% is montmorillonite: 20-60 mg Ca per litre of pore water 15-30 mg Mg 20-40 mg Na | 1.94 | 39 | 20 | $10^4$ | | percolation | $3.0\times10^{-11}$ | K. Pusch |
| | | | | $5\times10^3$ | | | $2.8\times10^{-11}$ | |
| | | | | $2\times10^3$ | | | $2.7\times10^{-11}$ | |
| | | | | $10^3$ | | | $2.7\times10^{-11}$ | |
| | 2.21 | 30 | 20 | $10^4$ | | | $5\times10^{-12}$ | |
| | | | | $2\times10^3$ | | | $5\times10^{-12}$ | |
| | 1.87 | 44 | 70 | $10^4$ | | | $3.1\times10^{-10}$ | |
| | | | | $2\times10^3$ | | | $3.1\times10^{-10}$ | |
| | | | | $10^3$ | | | $3.1\times10^{-10}$ | |
| | 1.93 | 37 | 70 | $5\times10^3$ | | | $9.0\times10^{-11}$ | |
| | | | | $2\times10^3$ | | | $8.0\times10^{-11}$ | |
| | | | | $10^3$ | | | $7.0\times10^{-11}$ | |
| | 2.13 | 29 | 70 | $10^4$ | | | $1.4\times10^{-11}$ | |
| | | | | $5\times10^3$ | | | $1.4\times10^{-11}$ | |
| 3. Na-Bentonite | 2.05 | | | $2.09\times10^5$ | 316 | | $6.7\times10^{-13}$ | Pacific North West Labs (Westsik et al) |
| | 2.13 | | | $1.56\times10^5$ | 766 | | $5.6\times10^{-13}$ | |
| 4. Ca-Bentonite | 2.09 | | | $2.13\times10^5$ | 858 | | $1.3\times10^{-12}$ | Pacific North West Labs |
| | 2.11 | | | $1.59\times10^5$ | 617 | | $1.6\times10^{-12}$ | |
| 5. 50% Na-Bentonite + 50% Sand (80-120 Mesh) | 2.12 | | | $1.62\times10^5$ | 192 | | $4.6\times10^{-12}$ | Pacific North West Labs |
| | | | | $7.18\times10^4$ | 46 | | $3.3\times10^{-12}$ | |
| | | | | $2.15\times10^5$ | 1011 | | $4.0\times10^{-12}$ | |
| | 2.09 | | | $1.73\times10^5$ | 618 | | $6.4\times10^{-12}$ | |
| 6. 25% Na-Bentonite + 75% Sand (80-120 Mesh) | 2.10 | | | $1.19\times10^4$ | 1222 | | $6.6\times10^{-10}$ | Pacific North West Labs |

TABLE IV (cont'd)

HYDRAULIC CONDUCTIVITY OF COMPACTED BENTONITE AND BENTONITE SAND MIXTURES
(From Literature Survey)

| Material | Specimen Characteristics | | Testing Conditions | | | | Hydraulic Conductivity cm/s | References & Remarks |
|---|---|---|---|---|---|---|---|---|
| | Dry Density $g/cm^3$ | M.C. % | Temp °C | Hyd. Grad. i | Test Duration (hrs) | Type of Test | | |
| 7. 50% volclay (MX-80) + 50% sand (80-120 mesh) + saline water | 2.22 | | | $1.66\times10^{5}$<br>$3.78\times10^{4}$<br>$2.27\times10^{5}$<br>$1.70\times10^{5}$ | | | $4.1\times10^{-12}$<br>$3.5\times10^{-12}$<br>$3.1\times10^{-12}$<br>$2.9\times10^{-12}$ | Pacific North West Labs |
| 8. Pure Bentonite and dionized water | 2.1± 0.04 | | 23<br>40<br>70<br>90 | | | | $(2.3\pm0.15)\times10^{-11}$<br>$(2.8\pm0.22)\times10^{-11}$<br>$(2.8\pm0.35)\times10^{-11}$<br>$(3.6\pm0.46)\times10^{-11}$ | Sandia Lab, (unpublished data) |
| 9. 30% Bentonite + 70% Sand to Brine B Water | 2.6± 0.1 | | 22<br>40<br>70<br>90 | | | | $(2.2\pm0.16)\times10^{-10}$<br>$(1.3\pm0.19)\times10^{-10}$<br>$(2.3\pm0.13)\times10^{-10}$<br>$(1.2\pm0.19)\times10^{-10}$ | Sandia Lab, (unpublished data) |
| 10. Yellow Wyoming Bentonite 8% Bentonite + 92% Lake Michigan Sand | | | | 1.3 m (hyd. head) | | Falling head<br>" "<br>(Tap Water) | $5.61\times10^{-8}$<br>$5.48\times10^{-8}$ | G.K. Alther |
| | | | | 1.0 m | | Constant head (Distilled Water) | $5.9\times10^{-8}$ | Average over 86 days with distilled water |
| 11. Blue Wyoming Bentonite (higher in Na content) 8% Bentonite + 92% Sand | | | | 1.3 m | | Falling head (Tap Water) | $2.79\times10^{-8}$<br>$2.46\times10^{-8}$ | Average over 86 days |
| | | | | 1.0 m | | Constant head (Distilled water) | $4.9\times10^{-8}$ | Average over 86 days |

R. Pusch, Properties of Bentonite Based Buffer Material. KBS-TR-32, 1978.

R. Pusch, Highly Compacted Sodium Bentonite for Isolated Rock Deposited Radioactive Waste Products. Nuclear Technology 45, 1979.

J.H. Westsik and L.A. Bray, F.N. Hodges and E.J. Wheelwright. Permeability, Swelling and Radionculides Retardation Properties of Candidate Backfill Materials. Pacific Northwest Laboratory, 1982.

National Sandia Laboratory Test Results, Progress Report. Personal Communication with Dr.M. Molecke of Sandia Laboratory.

G.R. Alther, The Role of Bentonite in Soil Sealing Applications. International Minerals and Chemical Corporation, Illinois, USA.

## TABLE V

HYDRAULIC CONDUCTIVITY TEST RESULTS FOR SEALBOND (ILLITE) BASED BUFFER ●

| Sample Identification | Mold/Compaction | Initial Moisture Content (%) | Dry Density ($kg/m^3$) | Porosity (%) | Degree of Saturation (%) | | Hydraulic Gradient | Pressure (kPa) | | k (cm/s) | | Remarks |
|---|---|---|---|---|---|---|---|---|---|---|---|---|
| | | | | | Initial | Final | | Inflow | Outflow | Inflow | Outflow | |
| CGS8-25* | Stainless steel mold, static compaction | 9.8 | 2112 | 20.0 | ~100** | ~100 | 70.3 | 70 | 35 | $1.5 \times 10^{-7}$ | $1.6 \times 10^{-7}$ | - |
| CGS8-25 | Stainless steel mold, static compaction | 8.8 | 2143 | 18.9 | ~100 | ~100 | 70.3 | 70 | 35 | $8.9 \times 10^{-8}$ | $1.2 \times 10^{-7}$ | - |
| CGS8-25 | Stainless steel mold, hand-compacted | 9.8 | 2072 | 21.6 | 94.2 | ~100 | 30.2<br>268.9 | 50<br>552 | 35<br>418 | $3.9 \times 10^{-8}$<br>$5.6 \times 10^{-8}$ | $3.5 \times 10^{-8}$<br>$5.6 \times 10^{-8}$ | - |
| CGS8-50 | Plexiglass mold, hand-compacted | 11.0 | 1980 | 24.9 | 87.9 | 91.3 | 70.3<br>70.3 | 70<br>280 | 35<br>245 | $6.9 \times 10^{-10}$<br>$3.1 \times 10^{-8}$ | $6.9 \times 10^{-10}$<br>$3.1 \times 10^{-8}$ | Small k due to higher saturation in soil. k increase probably due to higher back-pressure and air bubbles dissolved in water. |
| CGS8-50 | Stainless steel hand-compacted | 11.0 | 2021 | 24.4 | 91.2 | 95.6 | 70.3 | 70 | 35 | $4.7 \times 10^{-7}$ | $4.7 \times 10^{-7}$ | Sample dried at 120°C. Cracks developed in sample and between sample and mold. Sample re-wetted for 195 hours. |

* CGS8-25, Crushed Granite 75% mixed with Sealbond 25%

** Calculated degree of saturation was slightly more than 100% because of inaccuracies in volume, specific gravity and moisture measurements.

● H.S. Radhakrishna and H.T. Chan, Laboratory Study of Physical Properties of Clay Buffers for a Nuclear Fuel Waste Vault. Proc Int Conf on Radioactive Waste Management. CNS, Sept 1982.

## TABLE VI

### HYDRAULIC CONDUCTIVITY TEST RESULTS FOR PEMBINA BENTONITE BASED BUFFER [6]

| Sample Identification | Mold/Compaction | Initial Moisture Content (%) | Dry Density ($kg/m^3$) | Porosity (%) | Degree of Saturation (%) | | Hydraulic Gradient | Pressure (kPa) | | k (cm/s) | | Remarks |
|---|---|---|---|---|---|---|---|---|---|---|---|---|
| | | | | | Initial | Final | | Inflow | Outflow | Inflow | Outflow | |
| CGPB-25* | Stainless steel mold, sample hand-compacted | 14.6 | 1881 | 29.0 | 94.8 | ~100** | 30.2<br>277.0 | 50<br>552 | 35<br>415 | $2.1 \times 10^{-9}$<br>$3.7 \times 10^{-9}$ | $2.1 \times 10^{-9}$<br>$3.7 \times 10^{-9}$ | |
| CGPB-50 | Stainless steel mold, sample hand-compacted | 25.0 | 1560 | 41.0 | 96.9 | ~100 | 70.3<br>90.3<br>967.5 | 70<br>552<br>552 | 35<br>517<br>70 | -<br>$3.7 \times 10^{-10}$<br>$1.8 \times 10^{-10}$ | -<br>$4.7 \times 10^{-10}$<br>$1.9 \times 10^{-10}$ | Sample taking on water initially. |
| CGPB-50 | Stainless steel mold, sample hand-compacted | 25.0 | 1587 | 41.0 | 96.9 | 85.3 | 70.3<br>70.3 | 70<br>552 | 35<br>517 | $7.8 \times 10^{-10}$<br>$9.2 \times 10^{-9}$ | $2.7 \times 10^{-10}$<br>$9.0 \times 10^{-9}$ | Sample dried at 120°C. Rewetted for 200 hours, then hydraulic conductivity test. |

* CGPB-25 Crushed Granite 75% mixed with Pembina (calcium) Bentonite 25%

** Final degree of saturation was greater than 100% due to inaccuracies in measurements of volume, specific gravity, moisture content, etc.

[6] *H.S. Radhakrishna and H.T. Chan, Laboratory Study of Physical Properties of Clay Buffers for a Nuclear Fuel Waste Vault. Proc Int Conf on Radioactive Waste Management, CNS, Sept 1982.*

## TABLE VII

HYDRAULIC CONDUCTIVITY TEST RESULTS FOR BLACK HILLS BENTONITE BASED BUFFER ❶

| Sample Identification | Mold/Compaction | Initial Moisture Content (%) | Dry Density ($kg/m^3$) | Porosity (%) | Degree of Saturation (%) | | Hydraulic Gradient | Pressure (kPa) | | k (cm/s) | | Remarks |
|---|---|---|---|---|---|---|---|---|---|---|---|---|
| | | | | | Initial | Final | | Inflow | Outflow | Inflow | Outflow | |
| 10% Bentonite & 90% Silica Sand | Plexiglass mold, hand-compacted | 9.6 | 1845 | 30.5 | 58.0 | 91.4 | 277<br>555<br>832<br>139 | 138<br>276<br>413<br>69 | 0<br>0<br>0<br>0 | -<br>-<br>-<br>- | $3.1x10^{-10}$<br>$3.7x10^{-10}$<br>$3.4x10^{-10}$<br>$3.5x10^{-10}$ | - Flow rate could only be measured at the bottom end of the sample.<br>- First test in the program and the design of the permeameter was being modified at the time. |
| CGP8-25* | Plexiglass mold, hand-compacted | 16.5 | 1688 | 35.9 | 77.6 | 98.2 | 70.3<br>70.3 | 70<br>245 | 35<br>210 | $7.1x10^{-10}$<br>$1.3x10^{-9}$ | $6.5x10^{-11}$<br>$6.8x10^{-10}$ | - k (outflow) < k (inflow) because the sample was taking on water by swelling and this flow increased the "in-flow" and decreased the "outflow". |
| CGB8-25 | Stainless steel mold, static compaction | 14.6 | 1890 | 28.1 | 98.4 | ~100** | 555 | 552 | 276 | $1.3x10^{-10}$ | $1.1x10^{-10}$ | |
| CGB8-50 | Plexiglass mold, hand-compacted | 20.6 | 1647 | 38.1 | 899.1 | ~100 | 70.3 | 140 | 105 | $1.2x10^{-10}$ | $7.3x10^{-11}$ | |
| CGB8-50 | Stainless steel mold, static compaction | 18.0 | 1801 | 32.1 | 100 | ~ 100 | 832 | 552 | 138 | $3.7x10^{-11}$ | - | |
| CGB8-50 | Plexiglass mold, hand-compacted | 20.0 | 1676 | 36.9 | 90.9 | 95.0 | 70.3<br>70.3<br>282.0 | 140<br>245<br>400 | 105<br>205<br>260 | $1.1x10^{-10}$<br>$1.4x10^{-10}$<br>$7.4x10^{-11}$ | $5.3x10^{-11}$<br>$5.7x10^{-11}$<br>$6.4x10^{-11}$ | |
| CGB8-50 | Stainless steel mold, hand-compacted | 18.7 | 1549 | 41.7 | 69.4 | 94.1 | 1124.0 | 556 | 0 | $1.3x10^{-10}$ | $1.5x10^{-10}$ | - Sample dried at 120°C. Rewetted for 1800 hours. |

* CGB8-25 - Crushed Granite 75% + Black Hills Bentonite 25%

** Calculated degree of saturation was greater than 100% because of inaccuracies in volume, specific gravity and moisture content measurements.

❶H.S. Radhakrishna and H.T. Chan, Laboratory Study of Physical Properties of Clay Buffers for a Nuclear Fuel Waste Vault. Proc Int Conf on Radioactive Waste Management, CNS, Sept 1982.

TABLE VIII

SUMMARY OF $K_d$ VALUES FOR DIFFERENT RADIONUCLIDES

| Radionuclide | Th | | Np | | Tc | | Am | |
|---|---|---|---|---|---|---|---|---|
| Material | $K_d$ (mL/g) | Conditions (Reference) | $K_d$ (mL/g) | Conditions (Reference) | $K_d$ (mL/g) | Conditions (Reference) | $K_d$ (mL/g) | Conditions (Reference) |
| Illite (CEC = 14 meq 100 $g^{-1}$ (1)) | 120<br>$4 \times 10^3$ | pH = 3.7 (2)<br>pH = 7.0 (2) | 42 ± 4<br>13.6 ± 5.7<br>26.6 ± 1<br>295 ± 25 | 510 meq $L^{-1}$ NaCl; pH = 7 (4)<br>30 meq $L^{-1}$ $CaCl_2$; pH = 7 (4)<br>30 meq $L^{-1}$ NaCl; pH = 7 (4)<br>30 meq $L^{-1}$ $NaHCO_3$; natural (4) | 4.7 ± 0.5<br>0.5 ± 0.5<br>10.3 ± 1.1<br>0.0 ± 0.3 | 510 meq $L^{-1}$ NaCl; pH = 7 (4)<br>30 meq $L^{-1}$ $CaCl_2$ pH = 7 (4)<br>30 meq $L^{-1}$ NaCl; pH = 7 (4)<br>30 meq $L^{-1}$ $NaHCO_3$; natural (4) | | |
| Kaolinite (CEC = 5.0 meq 100 $g^{-1}$ (1)) | 600<br>$\sim 2 \times 10^5$ | pH = 3.0 (2)<br>pH = 6.2 (2) | 4.2 ± 1.8<br>0.5 ± 1.9<br>3.6 ± 2.0<br>122 ± 19 | as above | 0.4 ± 1<br>3.0 ± 5.3<br>0.4 ± 0.6<br>−0.2 ± 0.9 | as above | 4.3 | pH = 5;<br>0.25 mol/L Na (5) |
| Montmorillonite (CEC = 87 meq 100 $g^{-1}$ (1)) | $2 \times 10^3$<br>$2 \times 10^5$<br>$4 \times 10^4$ | pH = 5.5 (2)<br>pH = 7.9 (2)<br>pH = 6.5;<br>Ca-saturated (3) | 90.4 ± 7.0<br>17.4 ± 2.3<br>45.9 ± 4.9<br>9.1 ± 1.3 | as above | 0.2 ± 0.5<br>−0.6 ± 0.1<br>−0.6 ± 0.4<br>−1.5 ± 0.3 | as above | 33.9 | pH = 5;<br>0.25 mol/L Na (5) |
| Vermiculite (CEC = 77 meq $100^{-1}$ (1)) | | | | | 0.6 ± 0.7<br>−0.8 ± 0.3<br>0.4 ± 1.0<br>0.0 ± 0.2 | as above | | |
| Attapulgite | | | | | | | $3.04 \times 10^4$ | pH = 5;<br>0.25 mol/L Na (5) |
| Quartz (CEC = 0.13 meq 100 $g^{-1}$ (1)) | | | −0.1 ± 0.7<br>3.6 ± 2.3<br>4.1 ± 1.8<br>6.6 ± 4.3 | as above | 1.6 ± 0.9<br>0.7 ± 1.0<br>1.4 ± 1.5<br>−0.4 ± 0.3 | as above | | |

| Radionuclide | Ca | | Pu | | Sr | | Cs | |
|---|---|---|---|---|---|---|---|---|
| Material | $K_d$ (mL/g) | Conditions (Reference) | $K_d$ (mL/g) | Conditions (Reference) | $K_d$ (mL/g) | Conditions (Reference) | $K_d$ (mL/g) | Conditions (Reference) |
| Illite (CEC = 14 meq 100 $g^{-1}$ (1)) | | | 129 | pH = 5.9 (6) | 117<br>~ 200<br>~ 90<br>~ 2 | pH = 7.5 (6)<br>0.007 M $MgCl_2$; Mg-illite (7)<br>0.002 M $CaCl_2$; Ca-illite (7)<br>0.1 M $CaCl_2$; Ca-illite (7) | $2.86 \times 10^4$<br>$2.6 \times 10^5$<br>$2 \times 10^3$<br>$\sim 10^3$ | 0.1 M $CaCl_2$ (6)<br>distilled $H_2O$ (6)<br>K-illite (8)<br>Na-illite (8) |
| Kaolinite (CEC = 5.0 meq 100 $g^{-1}$ (1)) | 3.2 | pH = 5;<br>0.25 mol/L Na (5) | 352 | pH = 6.25 (6) | 55<br>257<br>~ 200<br>~ 1<br>~ 100 | pH = 7.5 (6)<br>pH = 10 (6)<br>0.0014 M $MgCl_2$ Ca-kaolin (7)<br>0.2 M $CaCl_2$ Ca-kaolin (7)<br>0.002 M $CaCl_2$; Ca-kaolin (7) | 94<br>$2.5 \times 10^3$<br>~ 900<br>~ 500 | 0.1 M NaCl (6)<br>distilled $H_2O$ (6)<br>Mg-kaolin (7) |
| Montmorillonite (CEC = 87 meq 100 $g^{-1}$ (1)) | 37 | pH = 5;<br>0.25 mol/L Na (5) | 630 | pH = 9.2 (6) | 506<br>~ 10<br>~ 700 | pH = 7.5 (6)<br>0.1 M $CaCl_2$; Ca-mont (7)<br>0.002 M $CaCl_2$; Ca-mont (7) | $2 \times 10^4$<br>$3 \times 10^3$ | K-mont (8)<br>Ca-mont (8) |
| Vermiculite (CEC = 77 meq $100^{-1}$ (1)) | | | $\sim 2 \times 10^5$<br>~ 250 | pH = 6.5; Ca-saturated<br>Pu(IV) (3)<br>pH = 6.5; Ca-saturated<br>Pu(VI) (3) | | | $2.7 \times 10^3$<br>$5.2 \times 10^4$ | 0.1 M NaCl (6)<br>distilled $H_2O$ (6) |
| Attapulgite | $1.38 \times 10^4$ | pH = 5;<br>0.25 mol/L Na (5) | $4.3 \times 10^3$ | pH = 9.6 (6) | | | | |
| Quartz (CEC = 0.13 meq 100 $g^{-1}$ (1)) | | | 0 | (6) | | | | |


1. R.J. Serne (Chairman), "Waste Isolation Safety Assessment Program Task and Contractor Information Meeting Proceedings, September 20-23", Battelle Pacific Northwest Laboratories Report, PNL-SA-6953 (1977).

2. S. Hansen, "The Behaviour in Underground Environments of Uranium and Thorium Discharged by the Nuclear Industry", IN: "Environment Behaviour of Radionuclides Released in the Nuclear Industry", International Atomic Energy Agency Report, IAEA-SM-172/55 (1973).

3. E.A. Bondietto, S.A. Reynolds and M.H. Shanks, "Interaction of Plutonium with Complexing Substances in Soils and Natural Waters", IN: "Transuranium Nuclides in the Environment", pp 273-287, International Atomic Energy Agency Report, IAEA-SM-199/51 (1975).

4. R.J. Serne, B. Rai, J.F. Relyea and M.J. Mason, "Batch $K_d$ Experiments with Common Minerals and Representative Ground Waters", IN: "Waste Isolation Safety Assessment Program Task and Contractor Information Meeting Proceedings, September 20-23", Battelle Pacific Northwest Laboratories Report, PNL-SA-6957 (1977).

5. G.W. Beall, B.M. Ketelle, R.G. Haire and G.D. O'Kelley, "Sorption Behaviour of Trivalent Actinides and Rare Earths on Clay Minerals" IN: "Radioactive Waste in Geologic Storage", ASC Symposium Series 100, p. 201-213 (1979).

6. T. Yamura, "Sorption Phenomena Significant in Radioactive-Waste Disposal", Mem. Amer. Ass. Petrol. Geol. 18, 318-330 (1973).

7. J.S. Wahlberg, J.M. Baker, R.W. Vernon and R.S. Dewar, "Exchange Adsorption of Strontium on Clay Minerals", U.S. Geological Survey Bulletin 1140-C, US Government Printing Office, Washington, 1962.

8. J.S. Wahlberg and Fishman, "Adsorption of Cesium on Clay Minerals", US Geological Survey Bulletin 1140-A, US Government Printing Office, Washington, 1962.

TABLE IX

RECOMMENDED RANGES AND VALUES FOR
SORPTION COEFFICIENTS FOR GRANITIC ROCKS ●

| Radionuclides | Recommended Ranges | | Recommended Values | |
|---|---|---|---|---|
| | $K_d$ (mL/g) | $K_a$ (cm)** | $K_d$ (mL/g) | $K_a$ (cm) |
| Tritium, T | - | - | 0 | 0 |
| Strontium, Sr | 0.6-600 | 0.2-2.2 | 10 | 0.7 |
| Zirconium, Zr | 1000-6000 | - | 1000 | 10 |
| Niobium, Nb | *-210 | 5-12 | 210 | 5 |
| Technetium, Tc | 0-80 | - | 26 | 0 |
| Ruthenium, Ru | *-200 | *-0.66 | 200 | 0.66 |
| Palladium, Pd | 0-28 | 0.4-1.1 | 11 | 0.7 |
| Cadmium, Cd | - | *-1.1 | - | 1.1 |
| Antimony, Sb | - | *-11 | - | 11 |
| Tellurium, Te | - | *-1.8 | - | 1.8 |
| Iodine, I | - | - | 0 | 0 |
| Cesium, Cs | 40-1000 | 0.6-5 | 100 | 0.6 |
| Cerium, Ce | 250-5000 | 2.2-16 | 1000 | 8 |
| Neodymium, Nd | 250-5000 | 2.2-16 | 1000 | 8 |
| Europium, Eu | 250-5000 | 2.2-16 | 1000 | 8 |
| Radium, Ra | 5-5000 | 1-18 | 80 | 6 |
| Thorium, Th | *-850 | - | 850 | - |
| Uranium, U | 0.4-10 | *-0.3 | 5 | 0.3 |
| Neptunium, Np | 40-100 | - | 80 | - |
| Plutonium, pu | 280-2000 | 4-500 | 280 | 4 |
| Americium, Am | 1000-$2 \times 10^4$ | 3.4-30 | 1000 | 8 |
| Curium, Cm | - | 5-24 | 1000 | 8 |

* Only one value available

** $K_a = K_d/SSA$ where SSA is in $cm^2/g$

● *T.T. Vandergraaf, A. Compilation of Sorption Coefficients of Radionuclides on Granites and Granitic Rock, AECL TR-120, 1982.*

## TABLE X

## SUMMARY OF GEOTECHNICAL CHARACTERISTICS OF SHAFT SEALING MATERIAL

| | Property | Required Characteristics |
|---|---|---|
| Physio-Chemical Properties | 1 - Hydraulic Conductivity | • Largest value of ($k_s$, $k_f$ and $k_i$) $\leq$ k of host rock (1) (see Figure 2)<br>• For evaluation of $k_s$ consider compositional and environmental factors<br>• For evaluation of $k_f$ direct in-situ measurement is most reliable approach, model analysis can be helpful<br>• $k_i$ is majorly controlled by state of stress within the seal mass and the seal-rock interface<br>• k of host granitic rock is highly dependant on site-specific conditions |
| | 2 - Sorption Capacity | • $K_{d(seal)} \geq (K_d$ or $K_a)$ rock (2)<br>• $K_d$ values depend on solid phase compositional factors and solution chemical and environmental conditions (see Tables 8 and 9)<br>• Large specific area (ion-exchange sites) of sealing material is a primary factor for its sorption capacity of radionuclides |
| Deformation Behaviour (Environmental Factors) | 3 - Compositional Factors | • Particles size and shape<br>• Type, valence and size of cations<br>• Pore-water chemistry (pH, ions concentration, etc) |
| | 4 - Density | • Compaction of seal material on dry side of optimum water content generally results in more favourable characteristics<br>• Laboratory investigations should determine the effects of density and degree of saturation on permeability, sorption coefficient, and compressibility |
| | 5 - Effects of Density, Temperature, and Chemical Environment on Volume Change | • Swelling pressure of a soil is controlled by its bulk density, pore-water chemistry and temperature<br>• Swelling potential is closely related to the clay fraction (plasticity) in a soil |
| | 6 - Compressibility and Cracking | • Compressibility is larger when material is compacted on wet side of optimum water content<br>• Broadly-graded soils are less compressible<br>• Arching action and separation of the seal from rock depend on seal's compressibility and volume change (swelling and shrinkage) characteristics and state of stress within the seal mass and the seal rock interface respectively |
| | 7 - Erosion and Piping | • Erosion and piping can hardly occur under anticipated natural and/or induced hydraulic gradients in the absence of arching action and/or interface opening |
| Thermal | 8 - Thermal Conductivity | • This is not a signficant factor, particularly at far-field.<br>• Placement of seal material at wet side of optimum water content can result in a higher thermal conductivity |
| Practicality | 9 - Other Considerations | • Materials availability.<br>• Emplacement practicality<br>• Economic feasibility |

(1) k, hydraulic conductivity of host formation
$k_s$, hydraulic conductivity of shaft seal
$k_f$, hydraulic conducitivity of disturbed rock
$k_i$, hydraulic conductivity of rock-seal interface

(2) $K_d$, seal or rock bed sorption coefficient
$K_a$, rock or fractures surface sorption coefficient

TABLE XI

HISTORICAL DEVELOPMENT IN EVALUATION OF AT-REST EARTH PRESSURE COEFFICIENT $K_o$

| Investigator | Values of $K_o$ | Test | Remarks |
|---|---|---|---|
| | $K_o = \frac{\sigma_h}{\sigma_v}$ at zero lateral deformation | — | Definition of concept |
| Terzaghi (1962) | Sand: $K_o$ = 0.42<br>Clay: $K_o$ = 0.70 to 0.75<br>(remolded, reconsolidated) | Metal-strip test | |
| Kjellman (1936) | Sand: 0.5 to 1.5 | One-dimensional triaxial compression test | $K_o$ is a function of stress history |
| Tschebotarioff and Welsh (1948) | Sand: 0.1 to 0.5<br>Blue Clay: 1.0 to 0.5 | Earth pressure meter | Effects of wall-friction and consolidation on $K_o$ |
| Bishop and Henkel (1962) | | $K_o$-triaxial test | $K_o$ depends upon the soil type, stress history and pore water pressure |
| Hendron (1963) | For the same $\phi$<br>$K_o$ (angular) ><br>$K_o$ (rounded) | High-pressure compression tests | Effect of particle shape on $K_o$ |
| Brooker and Ireland (1965) | Clays:<br>$K_o = 0.95 - \sin \phi'$<br>(for sands<br>$K_o = 1 - \sin \phi'$) | Modified Hendron test cell one-dimensional compression tests | The effects of $\phi'$, P.I., and stress history (OCR) on $K_o$ are studied |
| Ofer, Z., (1981) | $K_o$ (dry) = 0.34 to 0.43<br>Pd ≃ 13 kN/m³<br>$K_o$ (swelling) > 1<br>(montmorillonite clay) | Lateral soil pressure ring test (LSP MKII) | Effects of swelling and vertical pressure on $K_o$ |
| P.W. Mayne and F.H. Kulhawy, (1982) | $K_o = (1 - \sin \phi') \times \left[ \frac{OCR}{OCR_{max}^{(1-\sin \phi')}} + \frac{3}{4}\left(1 - \frac{OCR}{OCR_{max}}\right) \right]$ | Review of 170 different soils laboratory data | Relationship between $K_o$ and $\phi'$ and stress history by statistical analyses |

REFERENCES

Karl Terzaghi, Theoretical Soil Mechanics, John Wiley & Sons, Inc 1962.

W. Kjellman, Report on an apparatus for consummate investigation of the mechanical properties of soils. Proc 1st Int Conf on SM&FE, Vol 2, p 16, 1936.

G. Tschebotarioff and J.D. Welch, Effect of Boundary Conditions on Lateral Earth Pressures, Proc 2nd Int Conf on SM&FE, Vol 3, p 308, 1948.

Alan W. Bishop and D.J. Henkel, The Measurement of Soil Properties in the Triaxial Test, Edward Arnold (Publishers) Ltd, 1962.

Hendron, A.J., Jr, The Behaviour of Sand in One-Dimensional Compression, thesis presentation to the University of Illinois, at Urbana, Champaign, 1963 in partial fulfillment of the requirements for the degree of Doctor of Philosophy.

E.W. Brooker, and H.O. Ireland, Earth Pressures at Rest Related to Stress History, Canadian Geot Journ Vol II, No 1, 1965.

Zvi Ofer, Laboratory Instrument for Measuring Lateral Soil Pressure and Swelling Pressure, Geotechnical Testing Journ ASTM, Vol 4, No 4, Dec 1981, pp 177-182.

Paul M. Mayne and Fred H. Kulhawy, Ko-OCR Relationships in Soil, Journ of the Geot Eng Div, ASCE, Vol 108, No GT6, June 1982, pp 851-872.

TABLE XII

Summary of Studies and Case Records on
Arching Load Transfer in Clay Core of Zoned Dams

| Type of Study and/or Case Record | Relevant Conclusions | Remarks and References |
|---|---|---|
| Analysis by Finite Element Method (Elastic, Single Lift) | - position of maximum value of degree of arching ($d_a$) is not significantly influenced by stiffness ratio $k = E_A/E_B$ but extreme values of $d_a$ vary almost linearly with k<br>- degree of arching varies linearly with Poisson's ratio of backfill (core) for any value of k and position of maximum arching depends primarily on $\nu$. | - M. Moksimovic, 1973<br>- see Figure A.1 in Appendix for notations |
| Analysis by Finite Element Method (Plastic, Incremental Analysis) | - reduction in compressive stresses are influenced by molding water content (Poisson's ratio)<br>- potential cracking of clay core by hydraulic fracturing | - F.H. Kulhawy et al, 1976<br>- see Figure A.2 |
| Gepatsch Dam (153 m high, in Austria, built with vertical core in 1964) | - relief of vertical and lateral pressures due to arching is observed<br>- overall arching of dam is observed due to differential settlement | - W. Schober, 1967<br>- see Figure A.3 |
| Hyttejuvet Dam (93 m high dam built with very thin core in top half, in Norway, 1965) | - $\sigma_v \ll \gamma h$<br>- hypothesis of hydraulic fracturing is verified | - D.M. Wood et al, 1977<br>- see Figure A.4 |

TABLE XII (cont'd)

| Type of Study and/or Case Record | Relevant Conclusions | Remarks and References |
|---|---|---|
| Balderhead Dam (48 m high dam with vertical thin boulder-clay core, in England, 1965) | - reduction of effective stresses due to arching action correlates closely to the theoretical curve | - G.E. Blight, 1973<br>P.R. Vaughan et al, 1970<br>- see Figure A.5 |
| Holle and Harspranget Dams (40 m and 50 m high respectively, built in Sweden in 1950, with clay core placed against concrete diaphragm) | - reduction of total compressive stresses due to arching is quite compatible with theoretical results | - B. Löfquist, 1951<br>- E. Nonveiller and P. Anagností, 1961<br>- see Figures A.6 and A.7 |

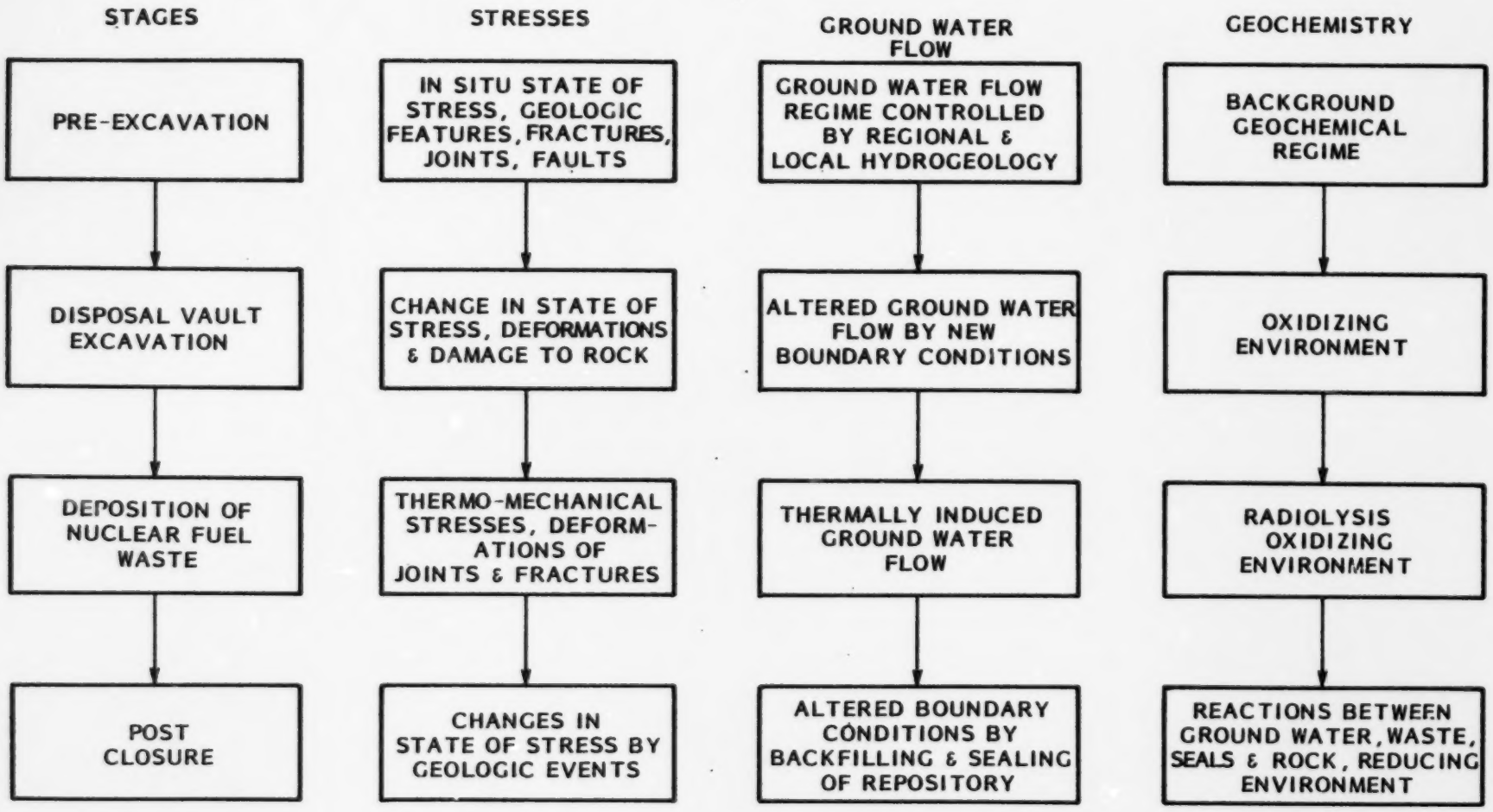
STAGES
STRESSES
GROUND WATER FLOW
GEOCHEMISTRY
PRE-EXCAVATION
IN SITU STATE OF STRESS, GEOLOGIC FEATURES, FRACTURES, JOINTS, FAULTS
GROUND WATER FLOW REGIME CONTROLLED BY REGIONAL & LOCAL HYDROGEOLOGY
BACKGROUND GEOCHEMICAL REGIME
DISPOSAL VAULT EXCAVATION
CHANGE IN STATE OF STRESS, DEFORMATIONS & DAMAGE TO ROCK
ALTERED GROUND WATER FLOW BY NEW BOUNDARY CONDITIONS
OXIDIZING ENVIRONMENT
DEPOSITION OF NUCLEAR FUEL WASTE
THERMO-MECHANICAL STRESSES, DEFORM-ATIONS OF JOINTS & FRACTURES
THERMALLY INDUCED GROUND WATER FLOW
RADIOLYSIS OXIDIZING ENVIRONMENT
POST CLOSURE
CHANGES IN STATE OF STRESS BY GEOLOGIC EVENTS
ALTERED BOUNDARY CONDITIONS BY BACKFILLING & SEALING OF REPOSITORY
REACTIONS BETWEEN GROUND WATER, WASTE, SEALS & ROCK, REDUCING ENVIRONMENT

FIGURE 1

ENVIRONMENTAL CONDITIONS IN A DISPOSAL VAULT DUE TO NATURAL AND INDUCED EFFECTS

166946 RD

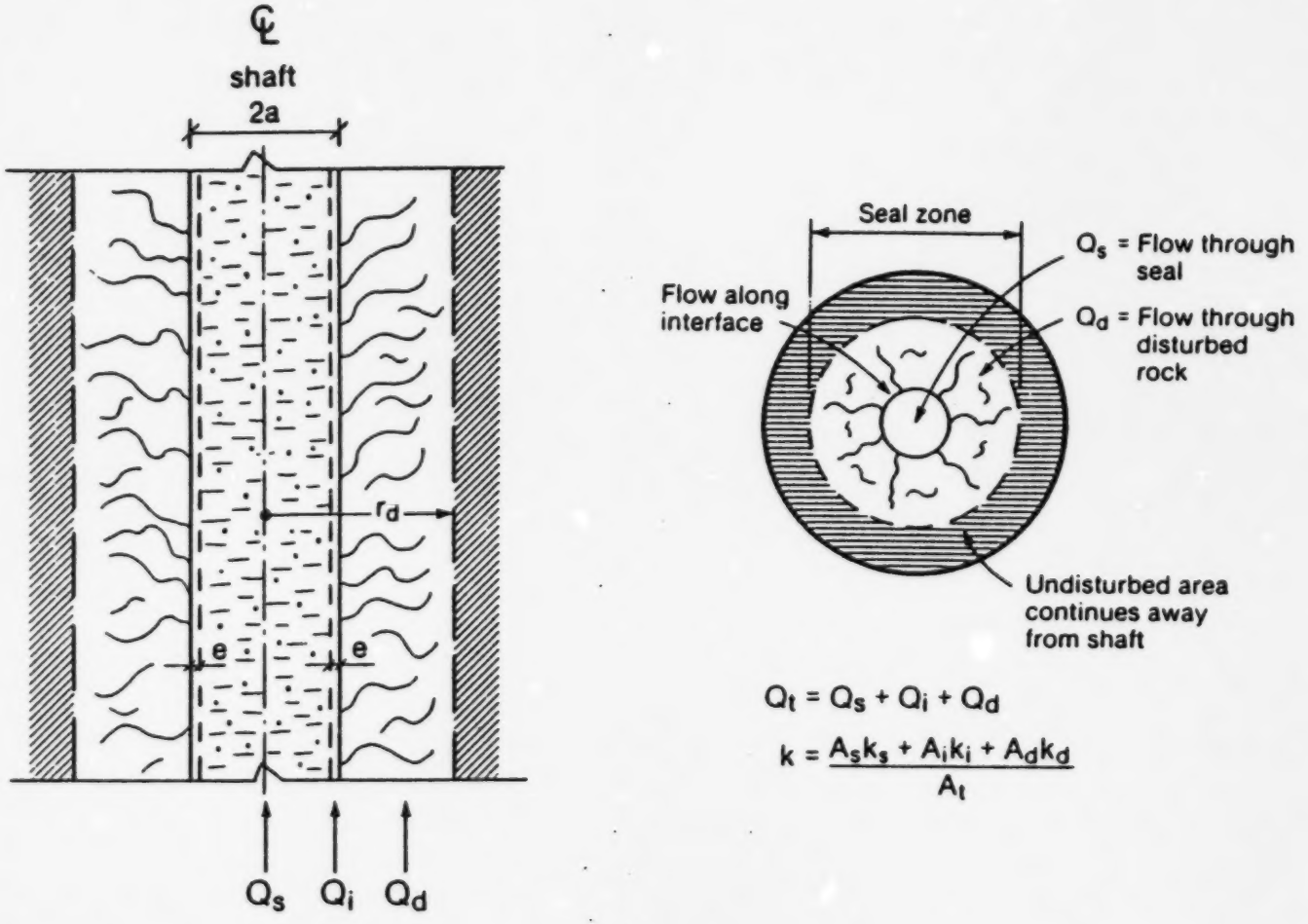


$$Q_t = Q_s + Q_i + Q_d$$

$$k = \frac{A_s k_s + A_i k_i + A_d k_d}{A_t}$$

FIGURE 2

POTENTIAL FLOW PATHWAYS THROUGH BACKFILLED SHAFT

164410 RD

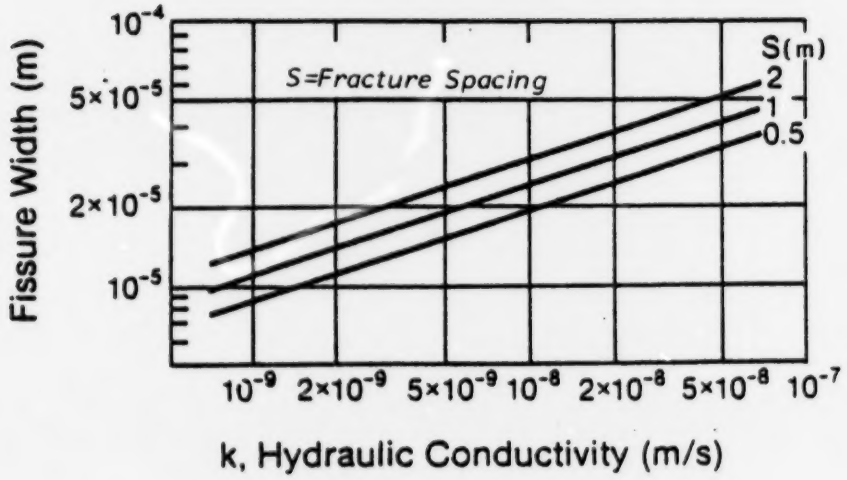


FIGURE 3

VARIATIONS OF HYDRAULIC CONDUCTIVITY WITH FISSURES OPENING AND SPACING. *

* *I. Neretnicks, Retardation of Escaping Nuclides from a Final Depository, KBS-TR-30, 1977.*

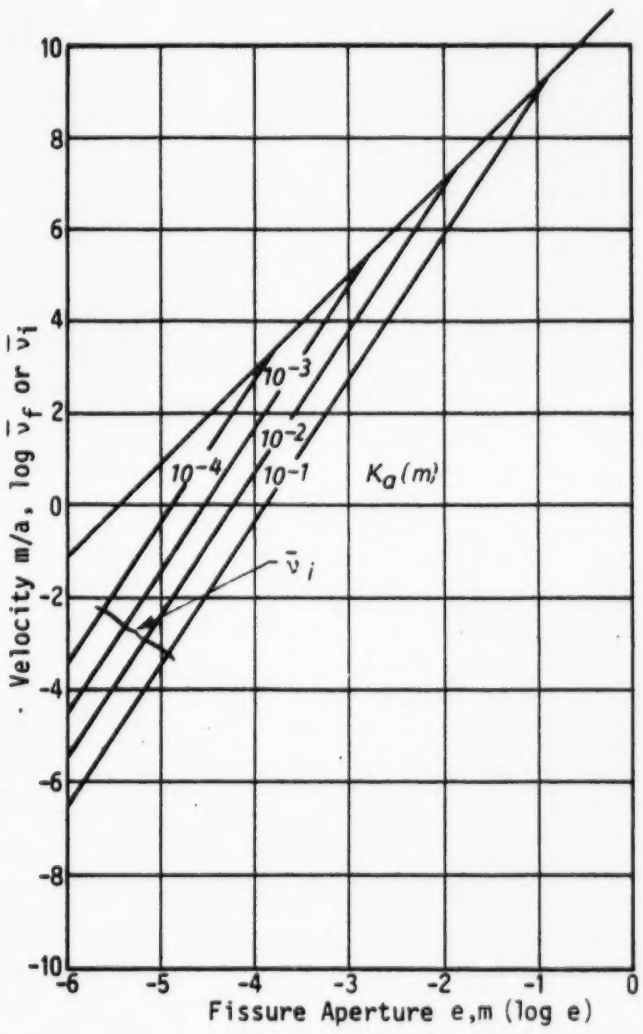


FIGURE 4

VARIATIONS OF WATER ($\bar{v}_f$) AND ION ($\bar{v}_i$) VELOCITIES IN FISSURED MEDIUM WITH FISSURE'S OPENING AND SURFACE EQUILIBRIUM CONSTANT $K_a$* (i=0,003m/m)

* *I. Neretnicks, Retardation of Escaping Nuclides from a Final Depository, KBS-TR-30, 1977.*

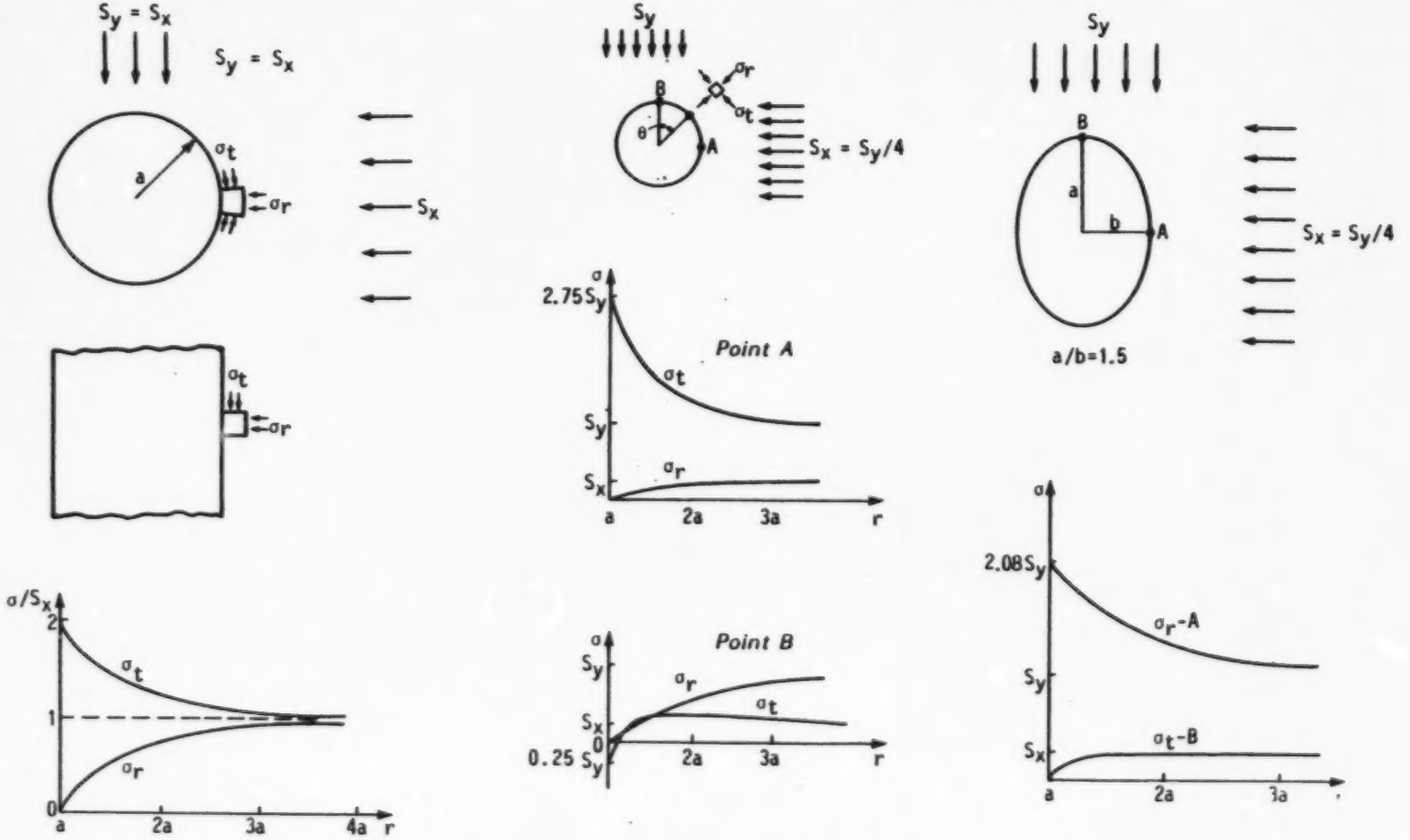


a) *Stress Variations with Distance from Circular Shaft in Uniform Stress Field*

b) *Stress Variations with Distance from Circular Shaft in Non-Uniform Stress Field*

c) *Stress Variations with Distance from Elliptical Shaft in Non-Uniform Stress Field*

**FIGURE 5**

**COMPARISON OF STRESS CONDITIONS AROUND SHAFTS OF DIFFERENT SHAPES AND DIFFERENT STRESS FIELD ***

* *D.F. Coates, Rock Mechanics Principles, Energy, Mines and Resources Can, Monograph 874 (Rev. 1981)*

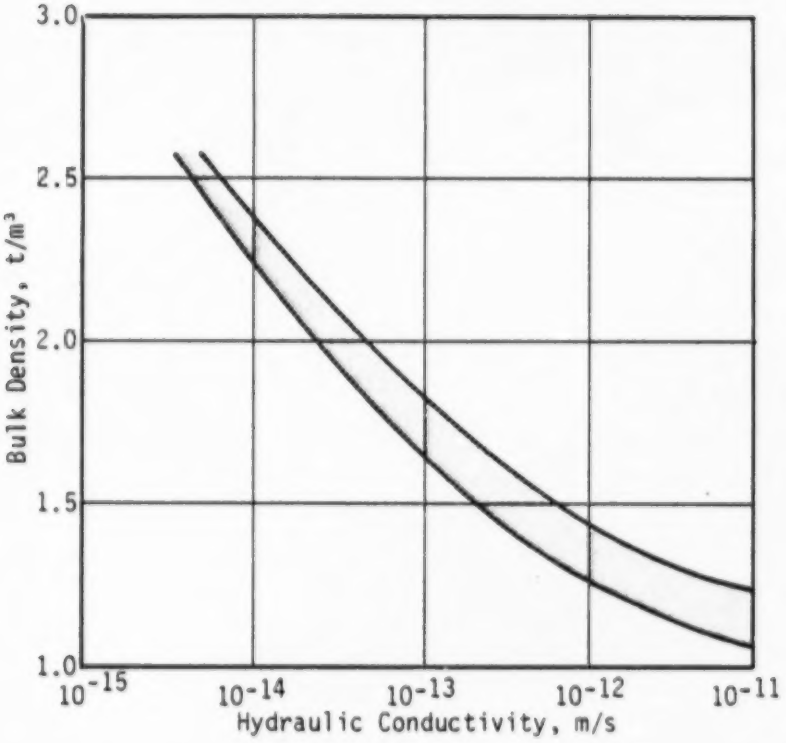


FIGURE 6

RELATIONSHIP BETWEEN BULK DENSITY AND HYDRAULIC CONDUCTIVITY OF NA-MONTMORILLONITE FROM LITERATURE SURVEY *

* *R. Pusch, Permeability of Highly Compacted Bentonite, KBS-80-16, 1980*

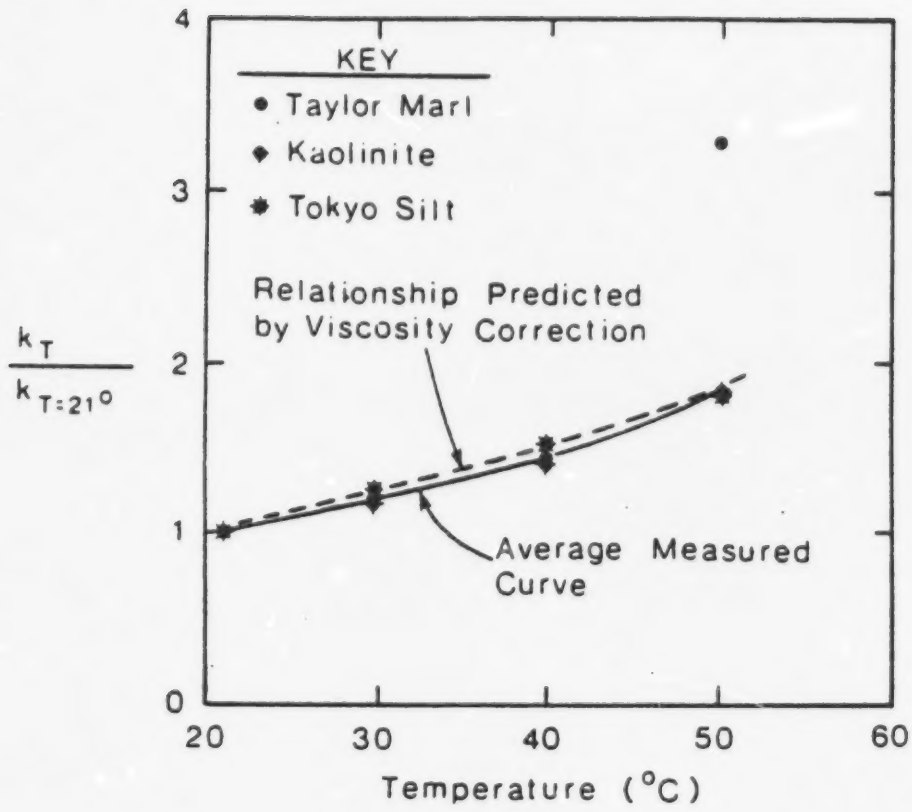


FIGURE 7

EFFECT OF TEMPERATURE ON PERMEABILITY. PERMEABILITY AT TEMPERATURE t($K_T$) ARE NORMALIZED WITH RESPECT TO THE MEASURED PERMEABILITY AT 21°C *

* *R.E. Olson and D.E. Daniel, Field and Laboratory Measurement of the Permeability of Saturated and Partially Saturated Fine-Grained Soils, June 1979, Geot. Engineering Report GR80-5, Dept. of Civil Engineering, University of Texas, Austin, Texas*

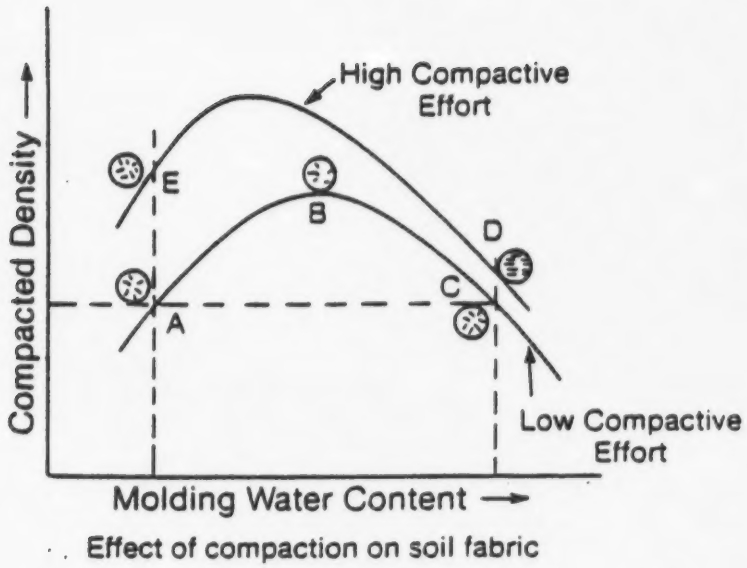


FIGURE 8a

EFFECT OF FABRIC ON THE HYDRAULIC CONDUCTIVITY OF COMPACTED CLAY SOILS *

* *T.W. Lamb, The Engineering Behaviour of Compacted Clay, J. Soil Mech. Found. Eng., ASCE (May), 1958*

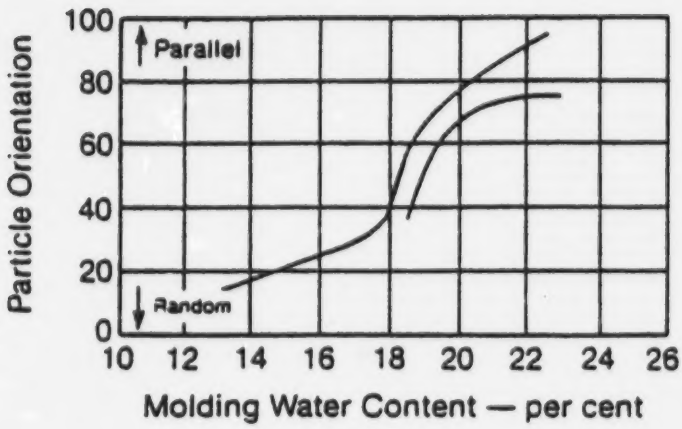


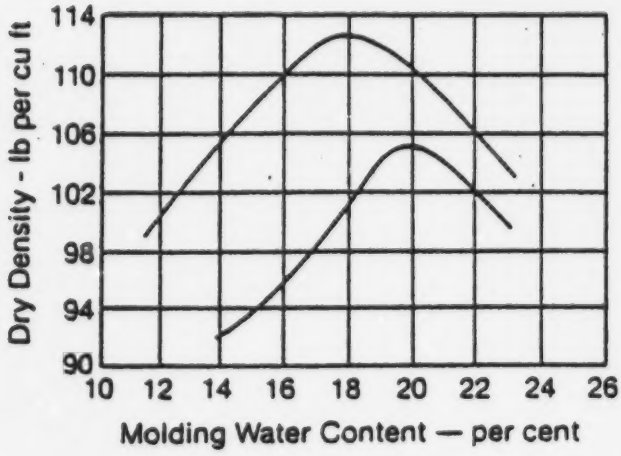


Influence of molding water content on particle orientation for compacted samples of Boston blue clay

FIGURE 8b

EFFECT OF FABRIC ON THE HYDRAULIC CONDUCTIVITY OF COMPACTED CLAY SOILS *

*J.G. Pacey, Jr., The Structure of Compacted Soils, SM Thesis, M.I.T., 1956

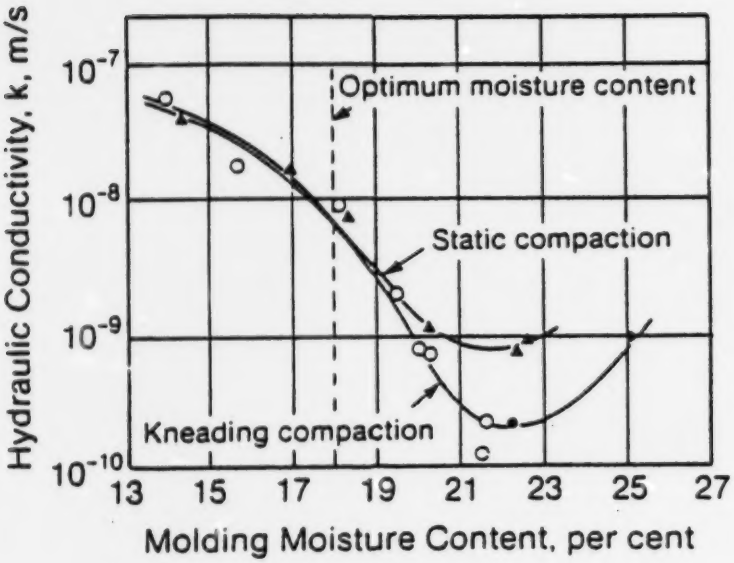


Effect of water content and compaction method on the hydraulic conductivity of a clay soil

FIGURE 8c

EFFECT OF FABRIC ON THE HYDRAULIC CONDUCTIVITY OF COMPACTED CLAY SOILS *

* *J.K. Mitchell, Fundamentals of Soil Behaviour, 1976*

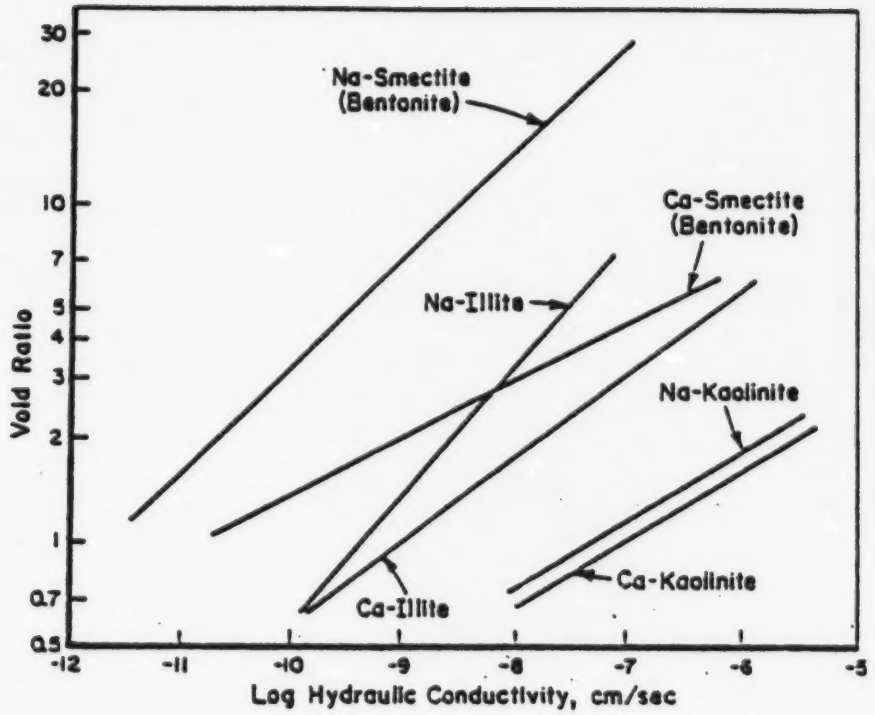


FIGURE 9

HYDRAULIC CONDUCTIVITY AS A FUNCTION OF VOID RATIO AND PORE FLUID CHEMISTRY FOR SEVERAL CLAYS*

* *G. Mesri and R.E. Olsen, Consolidation Characteristics of Montmorillonite, Geotechnique, Vol. 21, No. 4 PP. 341-352, 1971*

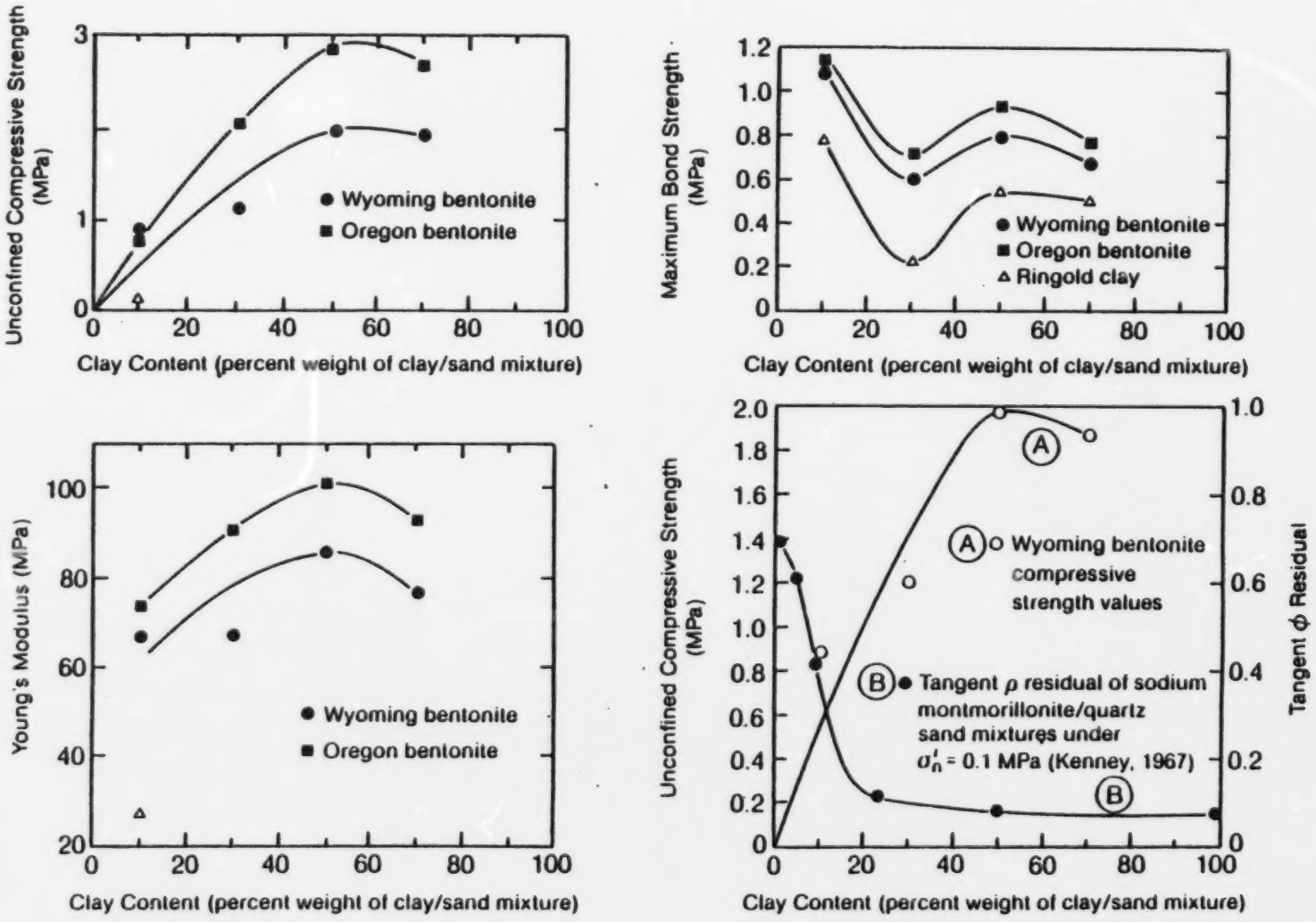
Unconfined Compressive Strength (MPa)
Wyoming bentonite
Oregon bentonite
Clay Content (percent weight of clay/sand mixture)
Maximum Bond Strength (MPa)
Wyoming bentonite
Oregon bentonite
Ringold clay
Clay Content (percent weight of clay/sand mixture)
Young's Modulus (MPa)
Wyoming bentonite
Oregon bentonite
Clay Content (percent weight of clay/sand mixture)
Unconfined Compressive Strength (MPa)
Tangent ϕ Residual
A
Wyoming bentonite compressive strength values
B
Tangent ρ residual of sodium montmorillonite/quartz sand mixtures under σ'n = 0.1 MPa (Kenney, 1967)
Clay Content (percent weight of clay/sand mixture)

FIGURE 10

RELATIONSHIPS BETWEEN STRENGTH PROPERTIES AND CLAY CONTENT OF CLAY-SAND MIXTURES

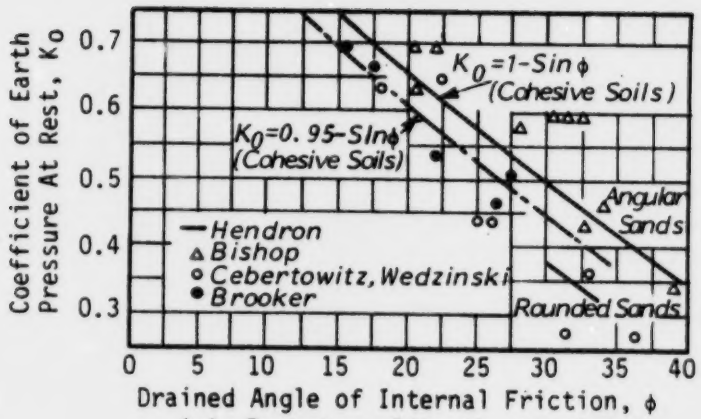


(a) Summary of $K_0$ Versus ϕ' Data

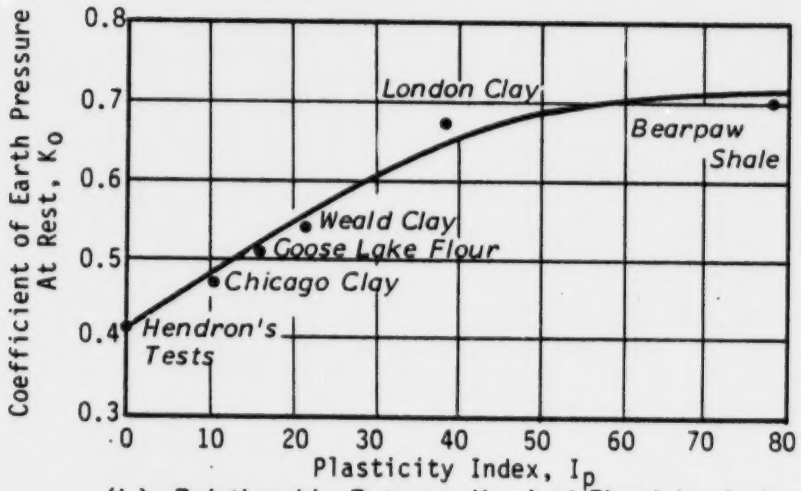


(b) Relationship Between $K_0$ And Plasticity Index For Normally Consolidated Clays

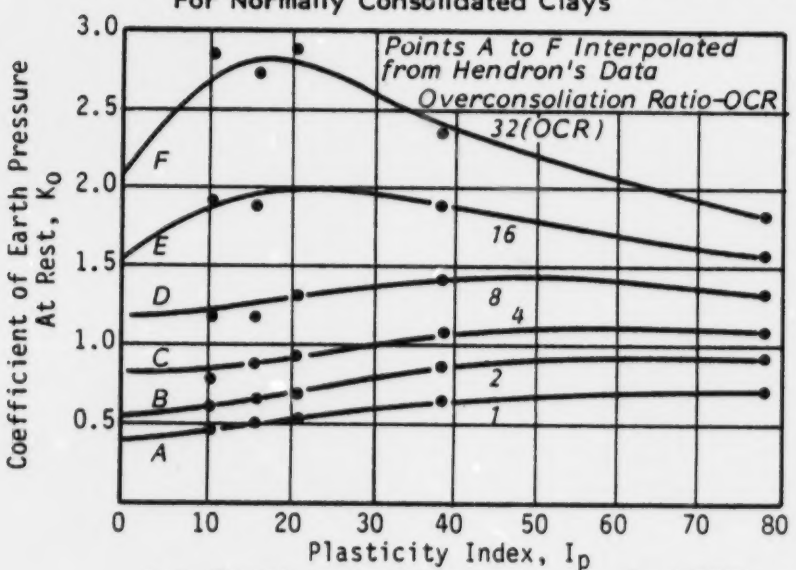


(c) Relationship Between $K_0$, $I_p$, And OCR

FIGURE 11

RELATIONSHIPS BETWEEN $K_0$, ϕ', PLASTICITY INDEX AND STRESS HISTORY *

* *E.W. Brooker and H.O. Ireland, Earth Pressure at Rest Related to Stress History, Can. Geot. J., Vol. II, No. 1, Feb. 1965*

164422 RD

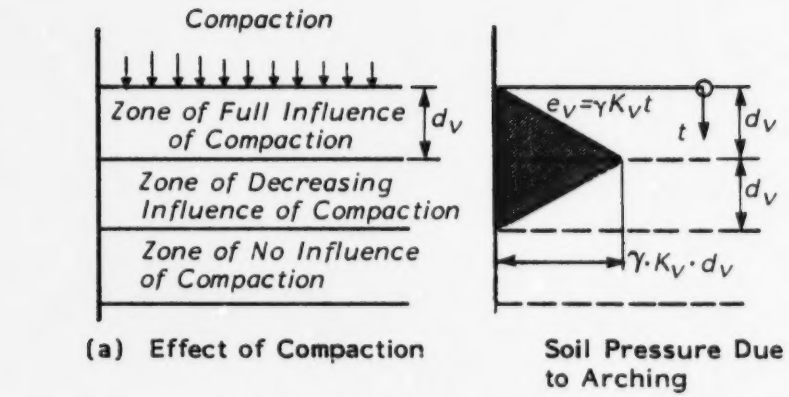


(a) Effect of Compaction

Soil Pressure Due to Arching

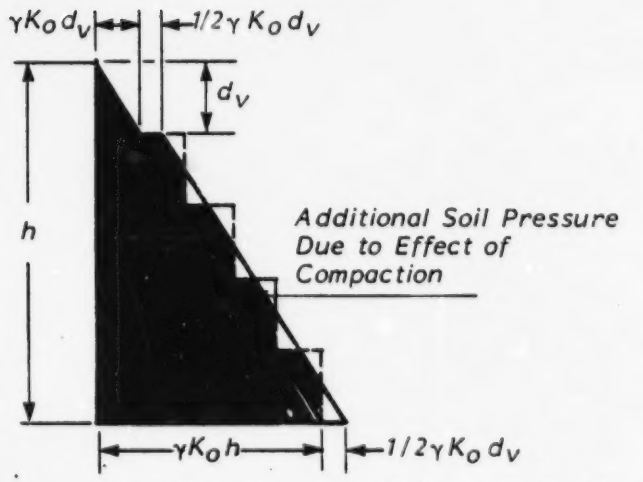


(b) $K_v \cong K_o$, Medium Compaction

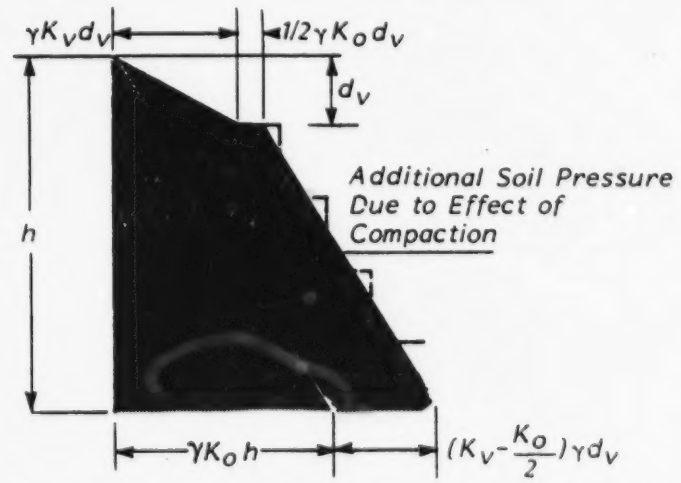


(c) $K_v \gg K_o$, Very High Compaction

FIGURE 12

SOIL PRESSURE DUE TO COMPACTION*

* *DIN 1055, Part 2, Design Loads for Buildings, Soil Properties, Unit Weight, Shear Resistance and Wall Friction, Translated from German by B. Lewicki, 1974*

164423 RD

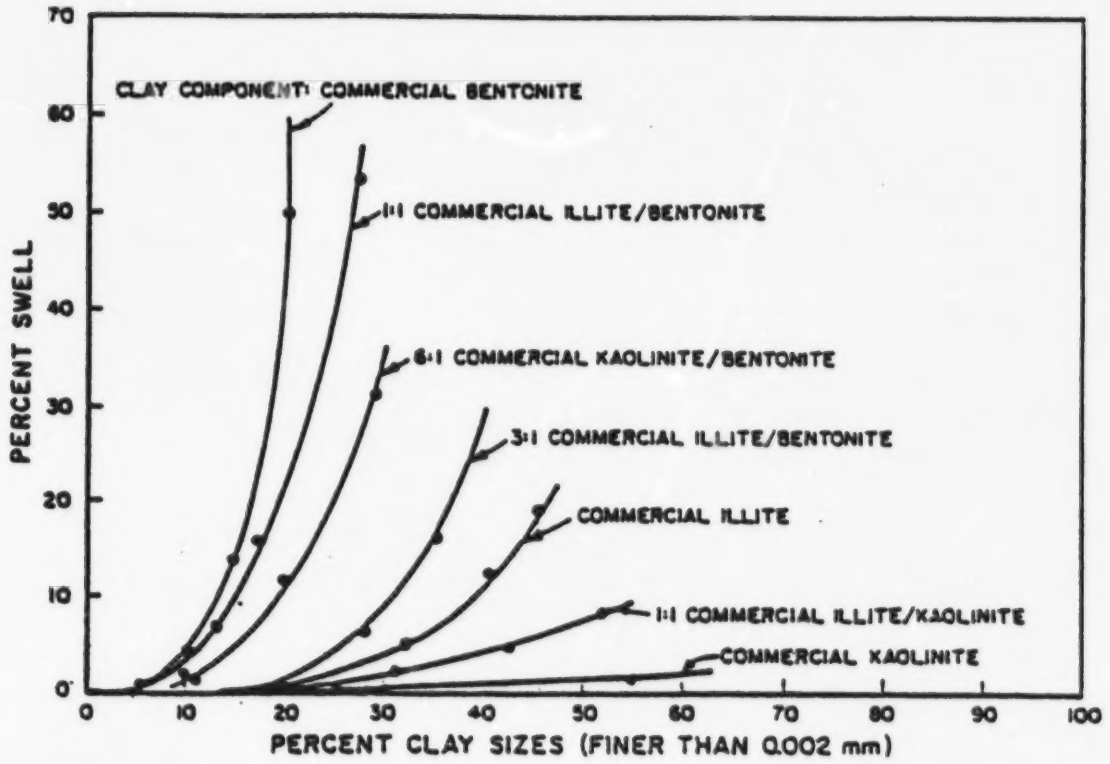


NOTE: PERCENT SWELL MEASURED UNDER 1 PSI SURCHARGE FOR SAMPLE COMPACTED AT OPTIMUM WATER CONTENT TO MAXIMUM DENSITY IN STANDARD AASHO TEST.

FIGURE 13

RELATIONSHIP BETWEEN PERCENTAGE SWELL AND PERCENTAGE OF CLAY SIZE PARTICLES FOR EXPERIMENTAL SOIL *

* *H.B. Seed, R.J. Woodward, and R. Lundgreen, Prediction of Swelling Potential for Compacted Clays. Journ. Soil Mechanics and Foundations Div., ASCE, Vol. 90, No. SM4, PP. 107-131, 1962*

| PROPERTY | KANDITES (K) (Kaoline. 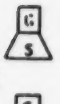 | G = Gibbsite sheet<br>S = Silica Sheet<br>K = Potassium ion<br>ILLITES (I) | SMECTITIES (S) (Montmorillonites) |
|---|---|---|---|
| Particle thickness, μm | 0.5-2 | 0.003-0.1 | ~0.001 (~10 Å) |
| Partical diam, μm | 0.5-4 | 0.5-10 | 0.5-1.0 |
| Specific surface, $m^2/g$ | 5-30 | 65-100 | 600-800 |
| Cation exchange capacity in meq/100 g (cec) | 3-15 | 10-40 | 80-150 |
| Compression Index, $C_c$ | ~0.2 | 0.6-1 | 1-3 |
| Liquid limit, $W_L$ | 30-70 | 60-120 | 150-700 |
| Plasticity Indix, $I_p$ | 20-40 | 30-65 | 100-650 |
| Activity, $A_c$ | 0.2 av. | 0.6 av. | 1-6 |
| $\phi'$ | $25^o$-$30^o$ | $20^o$-$25^o$ | $12^o$-$20^o$ |
| Swelling potential (see Figure D-3) | Very low | Medium | High |
| Other Characteristics | -Non-symmetrical unit structure, silt-sized stack<br>-Low water absorption (see Figure D-1)<br>-Specific gravity 2.63<br>-Rate of exchange reaction is instantaneous | -$K^+$ is not easily exchangable (correct size fitting) .'. stable<br>-Hydration ability is intermediate to that of Kandites, smectites<br>-Rate of exchange reaction is slow<br>-Specific gravity 2.64-2.69 | -cec is 80% due to lattice (isomorphous) substitution<br>-Non-liquid water thickness is 100 Å for Na(M) & 15 Å for Ca(M)<br>-Very high hydration ability<br>-Susceptible to illitization with contraction & liberation of water (@ T > 100°C) |
| Advantages (For use in disposal vault) | -Low compressibility<br>-High bearing capacity | -Chemical stability<br>-Low hydraulic conductivity<br>-Low swelling pressure | -Self-healing due to high plasticity and expansivity<br>-High sorption capacity due to large cec<br>-Low hydraulic conductivity |
| Disadvantages (For use in disposal vault) | -Large hydraulic conductivity<br>-Low sorption capacity<br>-Negligible expansivity and low plasticity | -Medium expansivity<br>-High compressibility<br>-Low sorption capacity | -High compressibility, Na(M)<br>-Low chemical stability<br>-Large swelling pressure |

FIGURE 14

SUMMARIZED PROPERTIES OF MAIN CLAY MINERAL GROUPS AND ADVANTAGES AND DISADVANTAGES OF THEIR USE IN DISPOSAL VAULTS

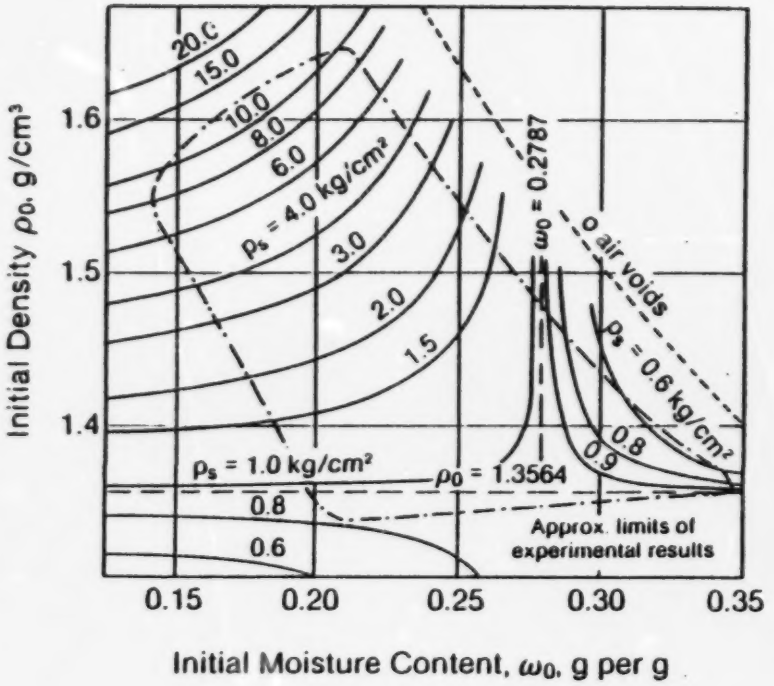


$$\rho = \rho(\rho_0, \omega_0, p, t)$$

where:

$\rho$ = final dry density
$\rho_0$ = initial dry density (1.35-1.65 g/cm³)
$\omega$ = initial water content (0.135-0.350 g/g)
p = applied surcharge (0.025-8 kg/cm²)
t = time (kept constant; 5 days)

$$\rho = a + b\rho_0 + c\omega_0 + dII + e\rho_0\omega_0 + f\omega_0 II$$

where:

a = 1.7882
b = -0.3154
c = -6.4116
d = 0.2117
e = 4.7193
f = -0.5532
$II = \log_{10}(P/1\ kg/cm^2)$
and correlation R = 0.9957

$$II_s = \log p_s = \frac{\rho_0(1 - b - e\omega_0) - c\omega_0 - a}{(d + f\omega_0)}$$

where by definition $\rho = \rho_0 @ P_s$

FIGURE 15

SWELLING PRESSURE $P_s$ AT VARIOUS INITIAL MOISTURE CONTENT AND INITIAL DENSITIES FOR A Ca-MONTMORILLONITE NATURAL CLAY (SEE FIG 16)*

* *A. Yevnin and D. Zaslarsky, Some Factors Affecting Compacted Clay Swelling, Can. Geotech. Journal, No. 7, 1970*

164426 RD

| Mechanical analysis (Hydrometer) | |
|---|---|
| Particles smaller than | % |
| 0.001 mm | 49.8 |
| 0.002 mm | 61.3 |
| 0.009 mm | 78.0 |
| 0.074 mm | 99.8 |
| 0.840 mm | 100.0 |

| Clay mineral composition of clay fraction smaller than 2μ (average of two tests) | |
|---|---|
| | % |
| Montmorillonite | 63 |
| Kaolinite | 14 |
| Illite | 13 |
| $Fe_2O_3$ | 4 |
| $Al_2O_3$ | 3 |
| $CaCO_3$ | 1 |
| $SiO_2$, etc. | 2 |
| | 100 |

(Some of the mineralogical tests are less accurate than others, and accuracy in % is only formal)

| | |
|---|---|
| Specific gravity | 2.77 g/cm³ |
| Plastic limit | 32% |
| Liquid limit | 64% |
| Plasticity index | 32% |
| Shrinkage limit | 10.2% |
| Maximum density (Proctor) | 1.385 g/cm³ |
| Optimum moisture content (Proctor) | 29% |
| Skempton's activity | 0.52 |
| pH | 7.7 |
| Organic matter (Carbon × 1.725) | 1.16% |
| $CaCO_3$ | 1% |

| Particles smaller than | Specific surface | Cation exchange capacity |
|---|---|---|
| | m²/g | me/100 g |
| 20 mesh sieve | 340 | 62.45 |
| 2μ | 550 | 84.0 |

| Exchangeable ions in material passing 20 mesh sieve | | |
|---|---|---|
| Ion | me/100 g | % |
| $Ca^{++}$ | 57.44 | 92.0 |
| $Mg^{++}$ | 2.93 | 4.7 |
| $Na^{+}$ | 1.067 | 1.7 |
| $K^{+}$ | 1.013 | 1.6 |
| Total | 62.45 | 100.0 |

FIGURE 16

PROPERTIES OF NATURAL CLAY SOIL TESTED FOR SWELLING BEHAVIOR

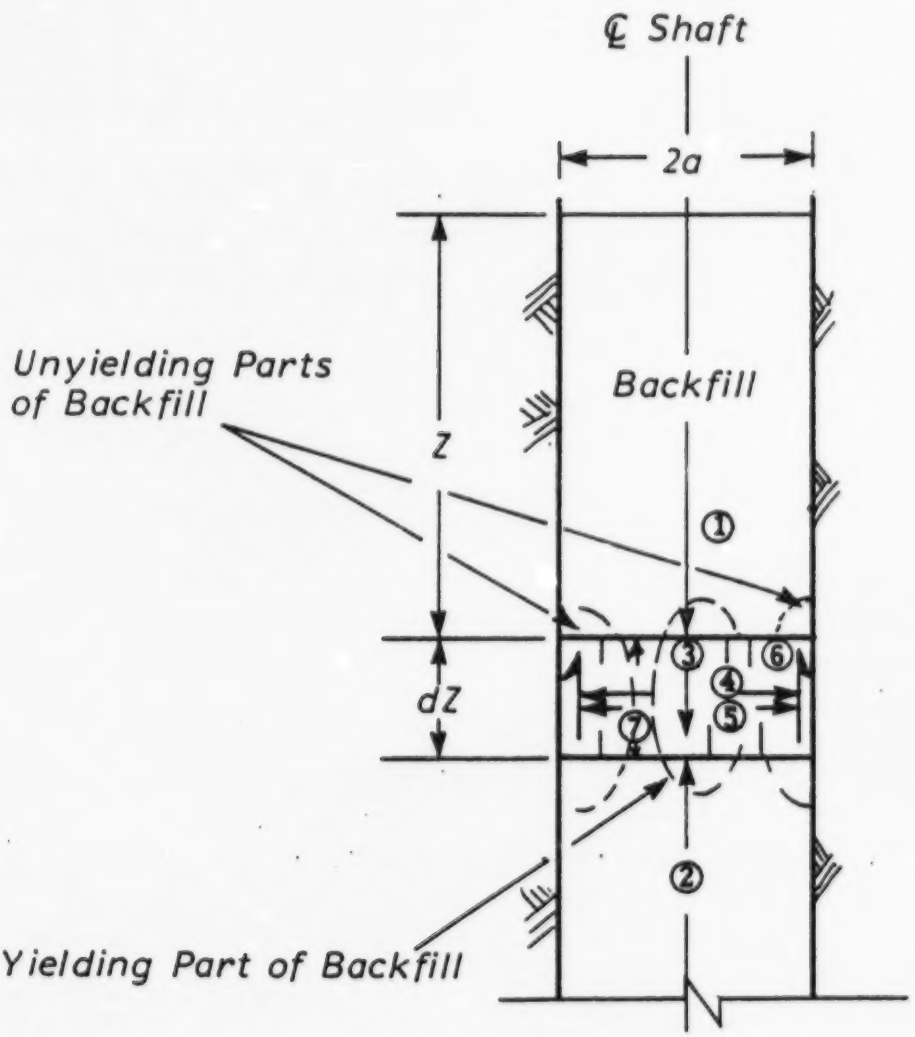


① = $\pi a^2 \sigma_v'$

② = $\pi a^2 (\sigma_v' + d\sigma_v')$

③ = $\pi a^2 \gamma dZ$

④ = $\sigma_h'$

⑤ = $P_{s(h)}$

⑥ = $S_b = 2\pi a \frac{\tau}{F} = \frac{(c_a' + \sigma_h' \tan\delta) 2\pi a}{F}$

⑦ = $P_{s(v)}$

FIGURE 17
STRESSES IN THE BACKFILLED SHAFT

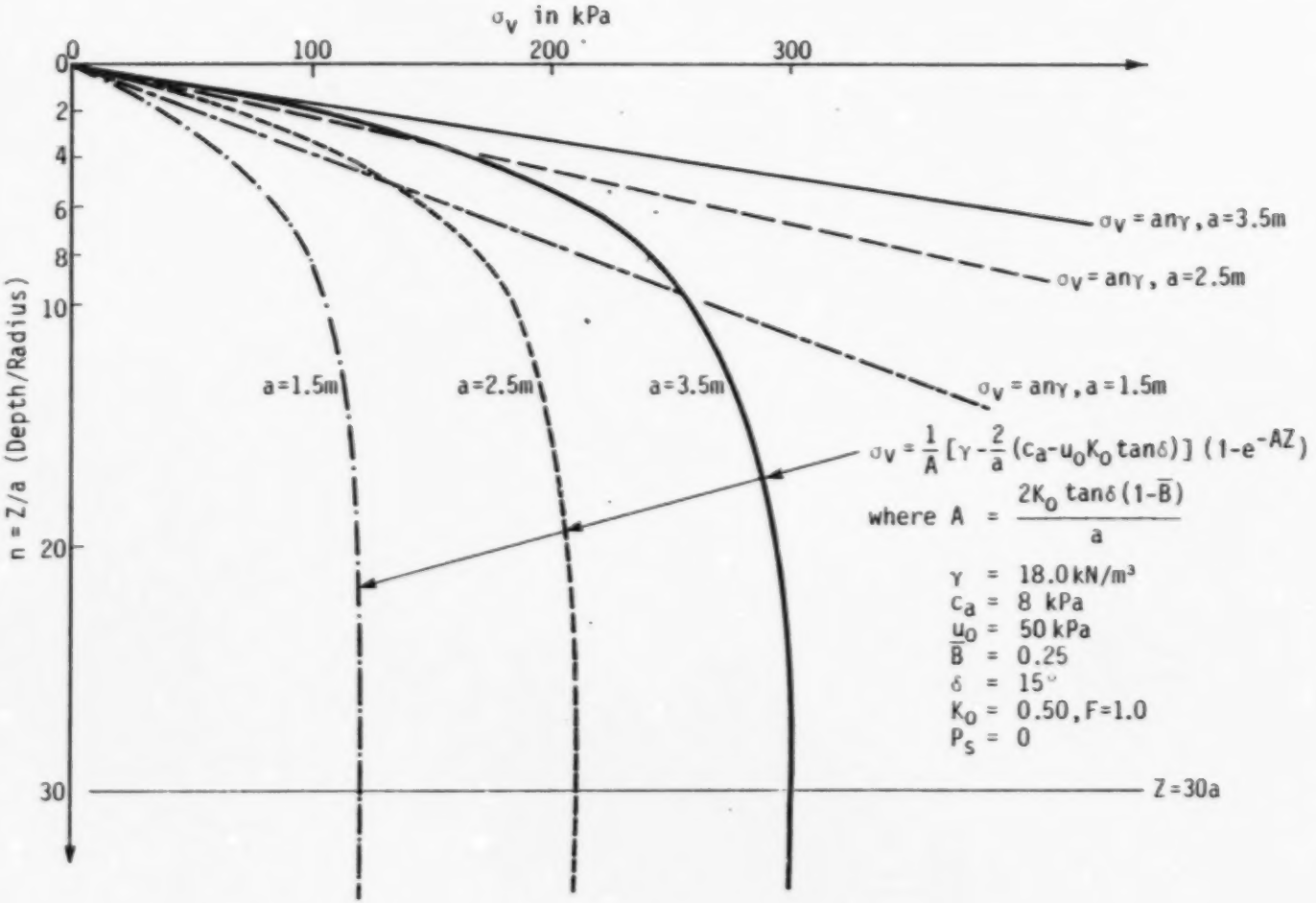


FIGURE 18

VARIATIONS OF VERTICAL STRESS IN A BACKFILLED SHAFT
DURING AND SHORTLY AFTER BACKFILL CONSTRUCTION

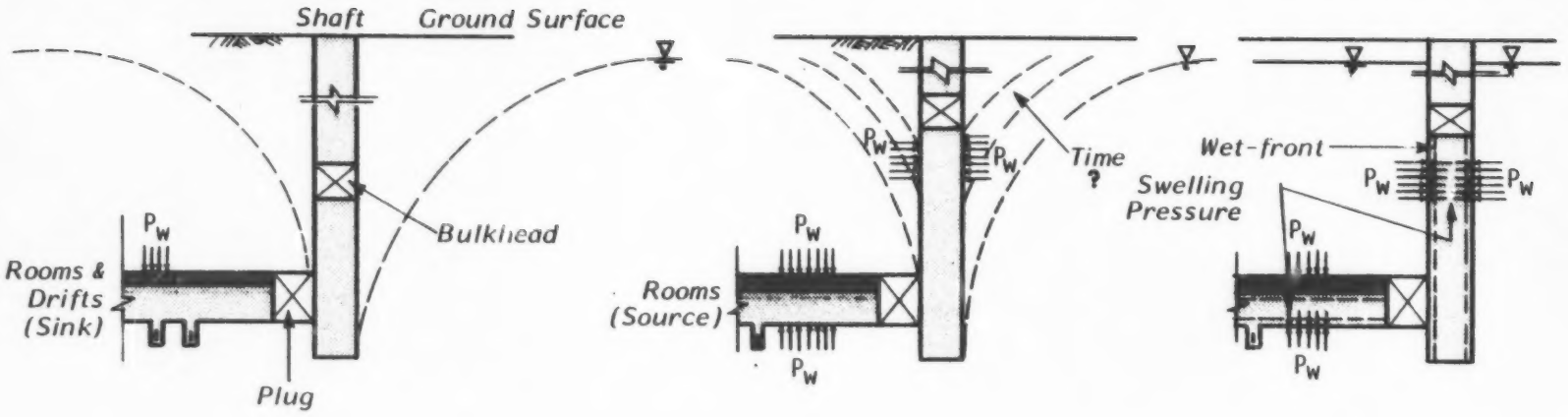


(a)
Construction
(Short-Term)

(b)
Ground Water Pressure Building Up
(Transition)

(c)
Backfill "Flooding"
(Long-Term)

FIGURE 19

DIFFERENT STAGES OF BACKFILLED EXCAVATIONS
IN A NUCLEAR FUEL WASTE DISPOSAL VAULT

164502 RD

APPENDIX

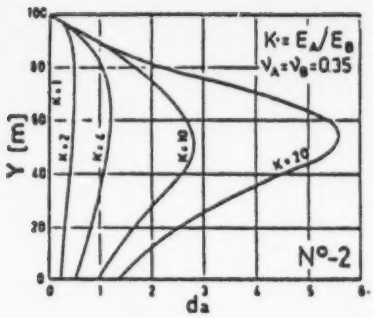


(a) Degrees of arching along the centerline of the core as a function of the stiffness ratio : $E_A/E_B = K$.

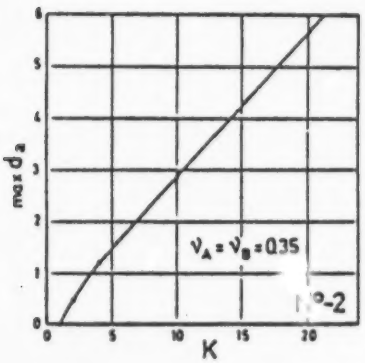


(b) Maximum values of degrees of arching as a function of stiffness ratio K.

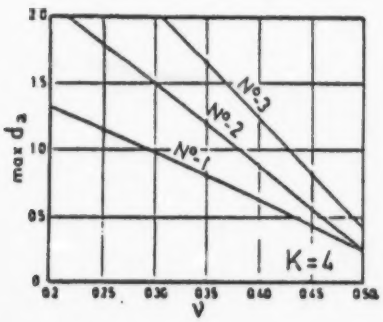


(c) Maximum values of the degree of arching as a function of Poisson's ratio for stiffness ratio K = 4.

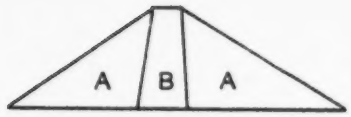


da: *"Degree of Arching"*

$$da = \frac{\sigma_{v(h)}}{\sigma_{v(n)}} - 1$$

*where:*

$\sigma_{v(h)}$ *is for homogeneous cross section,* $E_A = E_B$

$\sigma_{v(n)}$ *is for zoned (nonhomogeneous) cross section* $E_B \ll E_A$

$\rho$ = *Constant* = $2.0 t/m^3$

$E_A$ (Rockfill) = $2000 t/m^2$

$\nu_A = 0.35$

$E_B$, $\nu_B$ (core) } *Variable*

FIGURE A.1

INFLUENCE OF MATERIAL PROPERTIES ON DEGREE OF ARCHING (ALONG ℄ OF CORE)*

* *M. Maksimovic, "Optimum Position of the Central Clay Core of a Rockfill Dam in Respect to Arching and Hydraulic Fracture", Q.42, R.44, Congress on Large Dams, Madrid, PP. 789-799, 1973.*

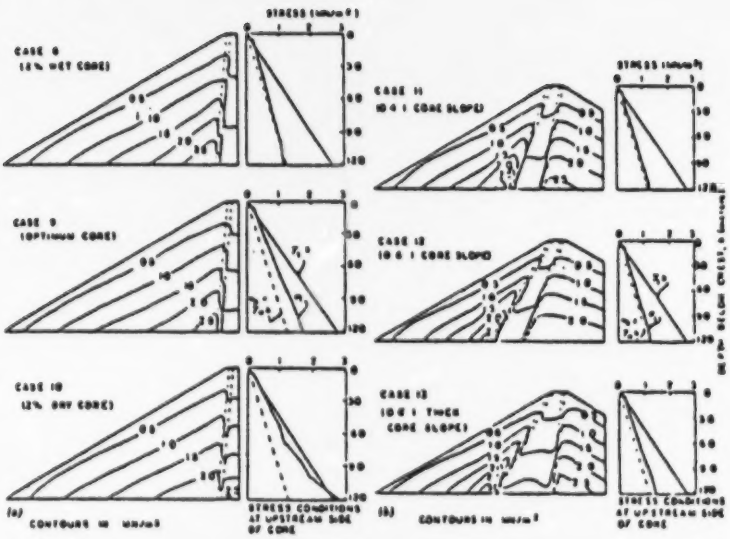

—Stress Conditions at Upstream Side of Core and Contours of Major Principal Stress in: (*a*) Cases 6, 9, and 10; (*b*) Cases 11, 12, and 13

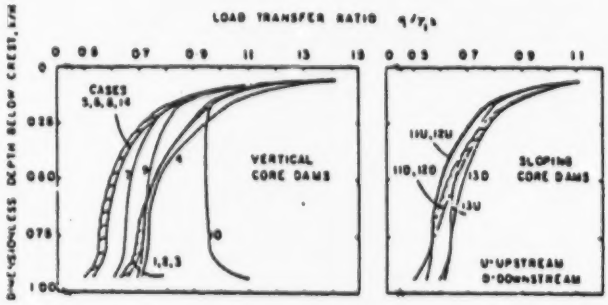


{ >1.0 *Load Transfer to Core from Shell*
{ <1.0 *Load Transfer from Core to Shell*

10 *Dry of Opt.*
9 *Opt.*
Others *Wet of Opt.*

4.—Variation of Load Transfer Ratio with Depth

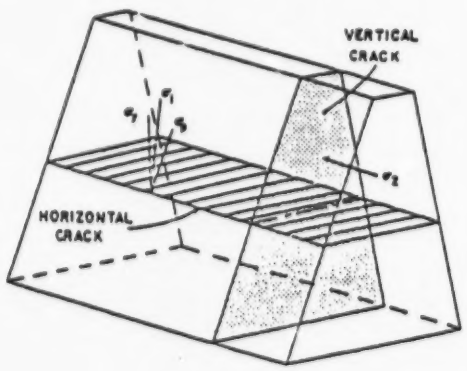


$\sigma_y$ = *Vertical Stress*
$\sigma_1$ = *Major Principal Stress*
$\sigma_p$ = *Stress II to Core Slope Face*

($\sigma_y$, $\sigma_1$, $\sigma_p$ *Differ by* ≤ 5%)

FIGURE A.2

POTENTIAL TRANSVERSE CRACKS AND ASSOCIATED STRESS CONDITIONS IN ZONED DAM CORES*

* *F.H. Kulhway and T.M. Gurlowski, Load Transfer and Hydraulic Fracturing in Zoned Dams, J. of Geol. Eng. ASCE, 102, GT 9, PP. 963-974, 1976*

GEPATSCH ROCKFILL DAM

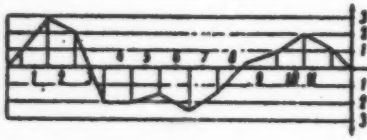


Expansion and Compression Along Dam Crest

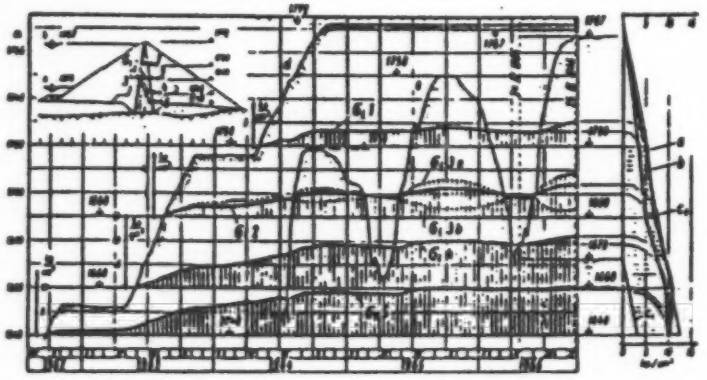

1-5 Soil pressure cells.
σ1-5 Side pressures at cells 1-5.
σ3a, 3b Side pressure at cell 3 with and without water pressure respectively.
a, b Side pressure on the downstream side for a reservoir level at 1673 and full level at 1767 respectively.
c1, c2 Water pressure for a reservoir level at 1673 and full level at 1767 respectively.
d Dam fill.
e Reservoir level.

Lateral Pressures on the Core Surface

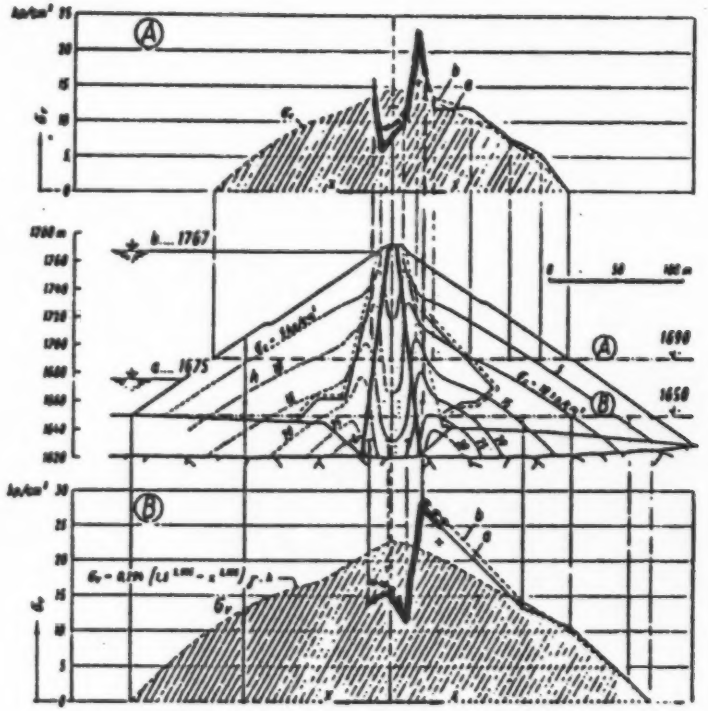

Vertical Soil Pressures at Level 1690 (A) or 1650 (B) as well as Isobars in the Main Dam Cross-Section.
a, b Pressure distribution measured for a reservoir level at 1675 and 1767 respectively (measuring values marked with a cross are the average of the readings for 2 cells).
σv Vertical pressure calculated. (E. Reinius)

Vertical Soil Pressures

FIGURE A.3

GEPATSCH DAM*
(153m high, 1964, Austria)

* *W. Schober, Behaviour of the Gepatsch Rockfill Dam, 9th Int. Congress on Large Dams, Q. 34, R. 39, Istamboul, 1867.*

164961 RD

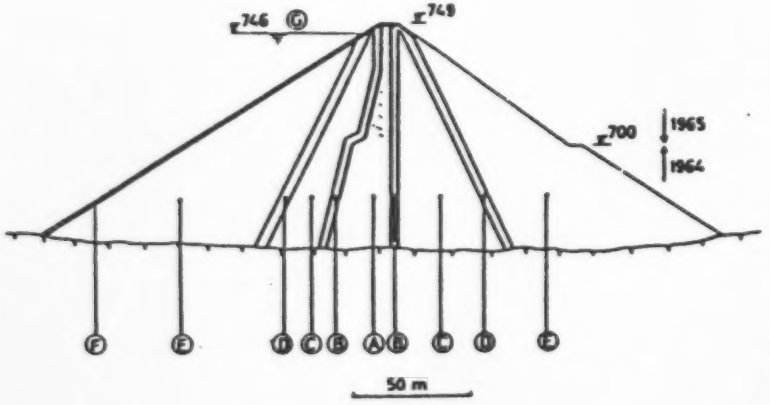


Transverse section of Hyttejuvet dam.

(A) Moraine
(B) Sandy gravel
(C) Gravel
(D) Tunnel spoil
(E) Quarried rock
(F) Quarried rock > 1/4 m³
(G) Maximum water level

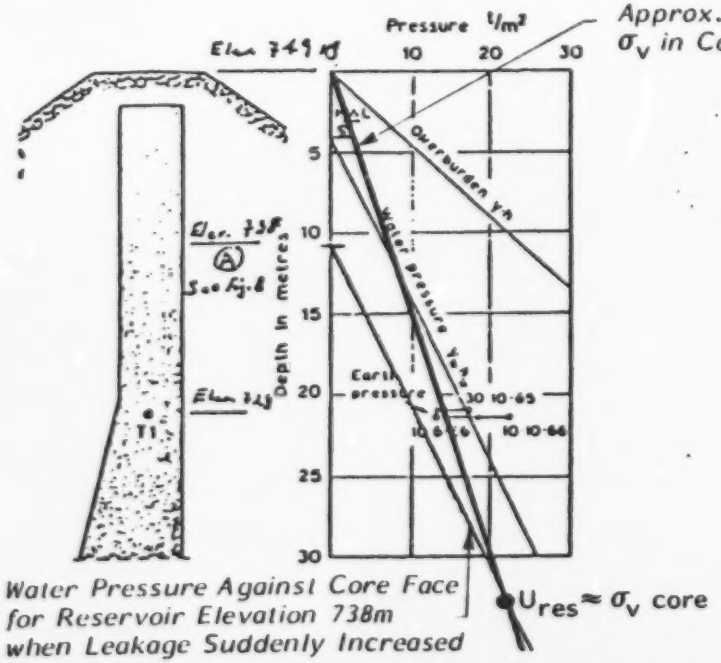


*Water Pressure Against Core Face for Reservoir Elevation 738m when Leakage Suddenly Increased*

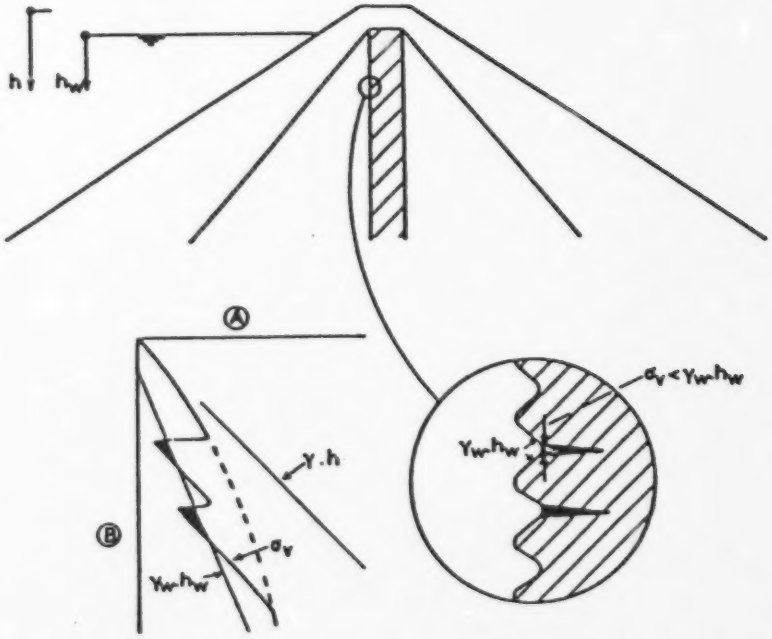


Outline of the hydraulic fracturing hypothesis used to explain the development of cracks in the core.
(A) Pressure (B) Depth

FIGURE A.4

HYTTEJUVET DAM*
(93m high, 1965, Norway)

* *D.M. Wood, B. Kjoernsli and K. Hoeg, Thoughts concerning the Unusual Behaviour of Hyttejuvet Dam. Norg. Geot. Inst. Pub. No.115, PP1-12, 1977*



85-13-184962 RD

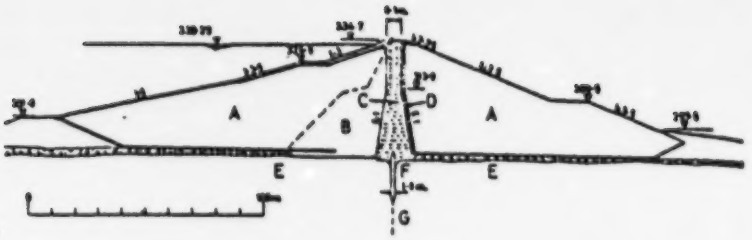


Cross section of dam at chainage 400 m.

(A) Shale fill.
(B) Fine shale fill.
(C) Boulder clay core.
(D) Crushed limestone filter.
(E) Shale foundation.
(F) Concrete cut-off.
(G) Grout curtain.

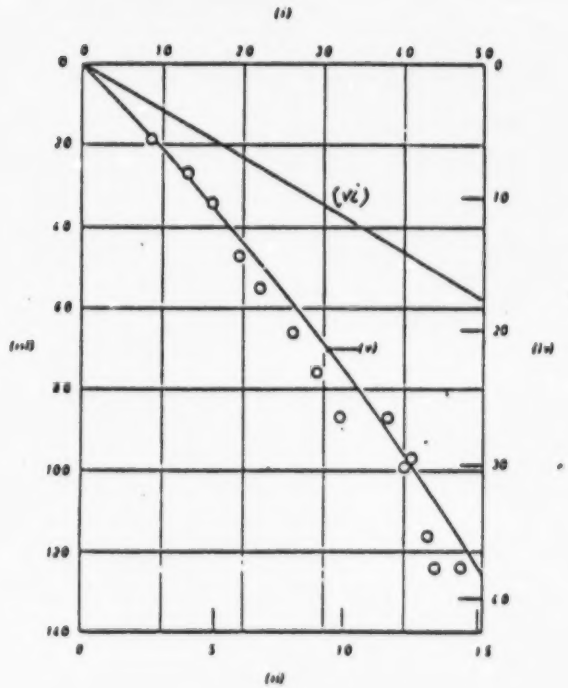


Comparison of Observed and Predicted Vertical Effective Stresses in the Clay Cores of Two Dams

(a) *Balderhead Dam*
(i) *Vertical Effective Stress* $\bar{\sigma}_v$ *in feet of fill*
(ii) *Vertical Effective Stress* $\bar{\sigma}_v$ *in metres of fill*
(iii) *Depth in feet*
(iv) *Depth in metres*
(v) *Predicted Profiles (based on Theoretical Arching effect)*
(vi) $\sigma'_v = \gamma h - u$ *(no Arching effect)*

FIGURE A.5

BALDERHEAD DAM*
(48m high, 1965, England)

* *G.E. Blight, Stresses in Narrow Cores and Core Trenches of Dams. Q.42, R.5, Congress on Large Dams, PP.63-79, 1973.*
* *P.R. Vaughan et al, Cracking and Erosion of the Rolled Clay Core of Balderhead Dam and the Remedial Works appointed for its Repairs, 10th Int. Congress on Large Dams, Q.36, R.5, Montreal, 1970.*

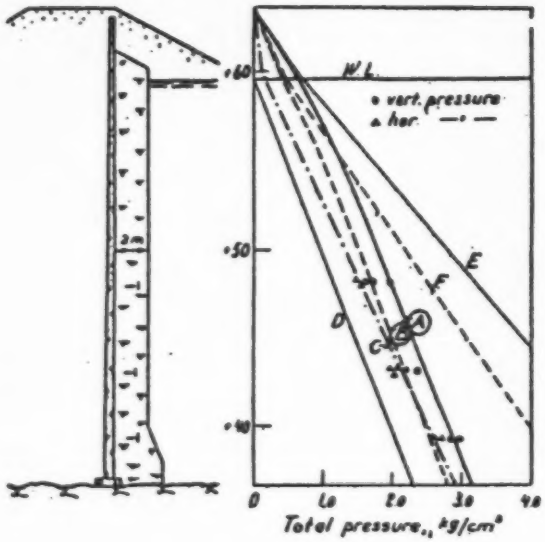


Earth pressure in the impervious layer at Hölle Dam after the latter had reached its full height.

*A and B.* Vertical pressure and horizontal pressure respectively according to eq. (1) ($\varphi = 12°$, $\gamma = 1.2$). — *C.* Active earth pressure from the upstream filling (moraine, $\varphi = 40°$, $\gamma = 1.1$). — *D.* Water pressure. — *E and F.* Vertical- and horizontal pressure respectively without taking the arching effect into account.

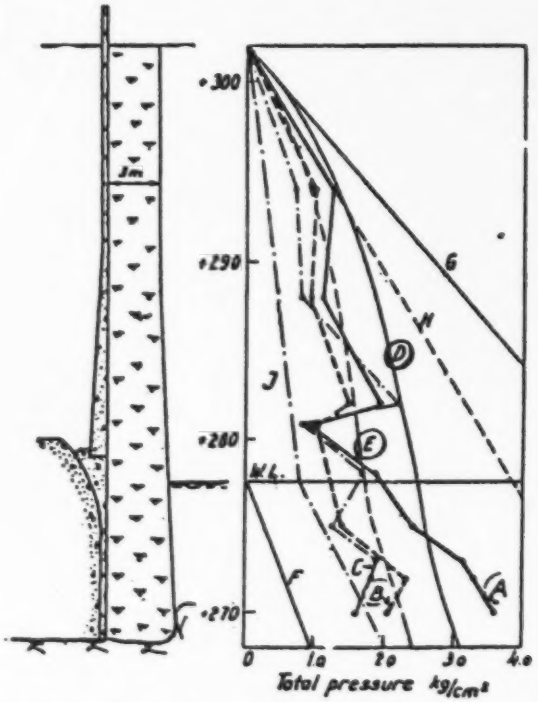


Earth pressure in the impervious layer at Harspringet Dam after the second seasonal filling.

*A.* Vertical pressure. — *B.* Horizontal pressure at right angles to the dam. — *C.* Horizontal pressure parallel to the dam. — *D and E.* Vertical- and horizontal pressure respectively calculated with respect to the arching effect ($\varphi = 10°$, $\gamma = 2.25$). — *F.* Water pressure. — *G and H.* Vertical- and horizontal pressure respectively calculated without taking the arching effect into account. — *J.* Active earth pressure from the upstream filling (rock filling $\varphi = 45°$).

Holle Dam (40m, 1949)

Harspranget Dam (50m, 1950)

FIGURE A.6

ARCHING EFFECT IN CLAY-CONCRETE CORE OF SWEDISH EARTH AND ROCK-FILL DAMS*

* *B. Lofquist, Earth Pressure in a Thin Impervious Core, Question No. 13, Congress on Large Dams, R.13, PP. 99-109, 1941*
*E. Nonveiller and P. Anagnosti, Stress and Deformations in Cores of Rockfill Dams, 5th I.C.S.M.F.E., Vol.II, PP. 673-680, 1951*

164964 RD

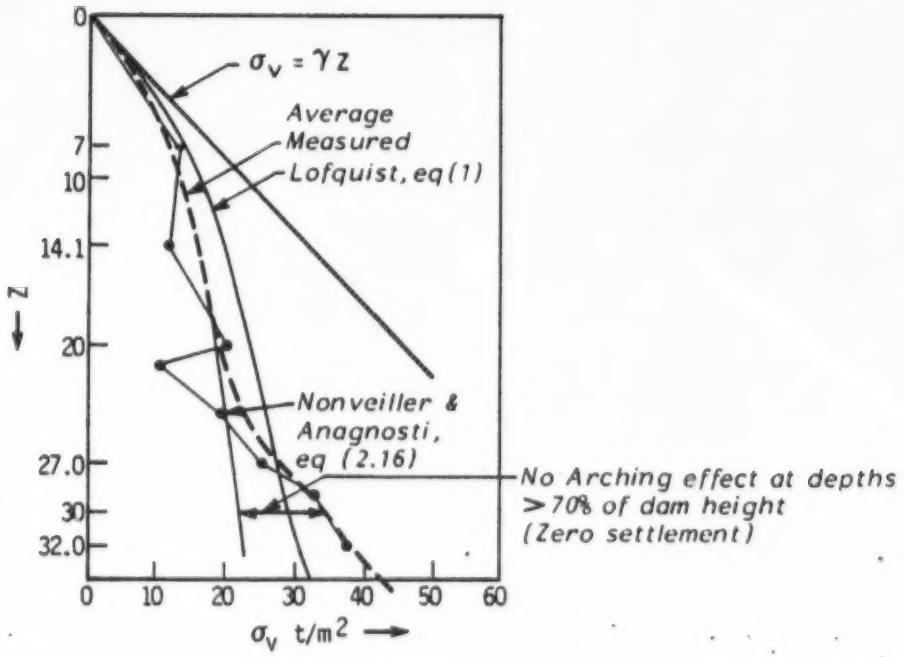


FIGURE A.7

ARCHING EFFECT AND COMPARISON OF MEASURED AND PREDICTED VALUES OF $\sigma_v$ IN THE CLAY CORE OF HARSPRANGET (SWEDEN)